

Alma Mater Studiorum – Università di Bologna

**DOTTORATO DI RICERCA IN
BIOINGEGNERIA**

Ciclo XXIV

Settore scientifico-disciplinare di afferenza:

ING-INF/06 BIOINGEGNERIA ELETTRONICA E INFORMATICA

Settore concorsuale di afferenza:

09/G2 BIOINGEGNERIA

**CT PERFUSION IMAGE PROCESSING:
ANALYSIS OF LIVER TUMORS**

Presentata da: Ing. Michela D'Antò

Coordinatore Dottorato

Prof. Angelo Cappello

Relatori

Prof. Mario Cesarelli

Prof. Claudio Lamberti

Prof. Paolo Bifulco

Ing. Maria Romano

Prof. Alessandra Bertoldo

Esame finale anno 2013

1. INTRODUCTION	5
1.1 Historical Highlights	5
1.2 Specific aims and work task	6
2. LIVER PERFUSION CT.....	10
2.1 Liver physiology	10
2.2 Basis of Perfusion CT	12
2.3 Perfusion CT assessment of hepatocellular carcinoma (HCC)	13
3. MATHEMATICAL MODELS FOR LIVER PERFUSION QUANTIFICATION WITH CT	17
3.1 Slope-ratio methods	17
3.1.1 Draining vein assumption method	18
3.1.2 No venous outflow method	19
3.1.3 Gradient method.....	21
3.2 Measurement of Blood Flow in the Liver with “Slope Method”; Problems and Proposed solutions.....	24
3.2.1 Time of Splenic Peak Method (also called “indirect approach”).....	24
3.2.2 Scaled Spleen Subtraction Method (also called “direct” approach)	26
3.2.3 Slope method: “combined approach”	27
3.3 “Dual input one compartment model”	28
3.4 “Deconvolution model”	29
4. ANALYSIS OF SOURCES OF VARIABILITY IN PERFUSION CT STUDIES.....	36
4.1 Choice of mathematical model.....	36
4.2 Imaging Studies used in this Thesis	37
4.3 Image processing method to derive perfusion parameters	40
4.3.1 Processing of time attenuation curves.....	40
4.3.2 Slope method analysis: influence of TAC processing	43
4.4 Comparison of maximum slope method and dual-input- one- compartment-model.....	53
5. SPV INDEX IN CHARACTERIZATION OF ARTERIAL HCC HYPERVASCULARIZATION	56
5.1 Standardized Perfusion Value: Historical background	56
5.2 Sources of Variability in the Use of Standardized Perfusion Value for HCC Studies	57
5.2.1 Material and Methods	58
5.2.2 Analysis of BFa Variability Due to ROI Manual Selection	58
5.2.3 Calibration of the CT System	59
5.2.4 Results	61

5.2.5	Discussion.....	62
5.2.6	Conclusion.....	65
6.	PERFUSION MAPS.....	66
6.1	Roi approach vs pixel by pixel approach: the value of perfusion map.....	66
6.2	Comparison of maximum slope method and dual-input-one- compartment-model: map based approach...	72
7.	CONCLUSION.....	75
	REFERENCES.....	77

1. INTRODUCTION

1.1 HISTORICAL HIGHLIGHTS

The extraordinary advances in medical technology over recent years have placed imaging at the centre of cancer diagnosis and assessment but today the information used to direct patient management is based almost entirely on morphological assessment. However, because of the wide spread of studies and the increasing interest, functional data will become an integral component of routine tumour imaging.

It is well recognized that a tumour cannot grow without a blood supply and that assessment of tumour vasculature provides a measure of tumour aggressiveness as well as insight into other factors related to prognosis, prediction of response to treatment and risk of recurrence. There are a lot of functional techniques employed in tumour clinical management but multidetector CT (MDCT) is widely spread for staging tumours and indeed remains the workhorse of cancer imaging today. Computed Tomography imaging is a standardized technique used in radiology to visualize the anatomical structures of the liver and its state of pathology, such as liver tumours. Currently, perfusion CT has become the most interesting technique for the quantitative study of liver tumour angiogenesis. The perfusion CT, a technique which require acquisition of image during contrast agent injection without table movement, allows to quantify important hemodynamic parameters that play an important role in diagnosis and staging of liver tumours.

This thesis is presented in the environment of liver cancer imaging improvement by the analysis and application of image processing techniques to liver perfusion CT.

Hepatocellular carcinoma (HCC) is the most common malignant liver tumour and is one of the most common tumours in the world, causing about 1 million deaths per year. It is well known that liver tumour tissue is characterized by an increased blood supply related to neoangiogenesis. This process is related with an increase of contrast enhancement on perfusion CT liver images.

Furthermore, primitive liver tumour (HCC) diagnosis, assessment and staging are critical because PET (Positron emission tomography), that represent the gold standard functional technique, is not a useful tool in the diagnosis and follow up of HCC, because metabolism of glucose in primitive liver tumour is not different from the surrounding liver parenchima. So liver perfusion CT studies are increasingly advocated as a means to assess the grade of vascularization in HCC patients and to evaluate variations in perfusion parameters following locoregional treatments or antiangiogenic drugs.

1.2 SPECIFIC AIMS AND WORK TASK

The specific aims at the start of the Ph.D. candidature were to:

- Investigate the basic principles and physics of liver perfusion CT technique
- Investigate the main mathematical modelling used to derive liver perfusion parameters
- Investigate image processing methods to derive perfusion parameters and perfusion maps
- Assess perfusion parameters variability related to different image processing methods
- Assess the value of Standardized Perfusion Value, which represents a new perfusion parameter, in characterization of arterial HCC vascularisation and generate SPV maps

In clinical application of perfusion CT imaging, there are a lot of technical limits, mainly in image processing analysis, some intrinsic and others operator-related.

So one of the most crucial steps in adopting this technique is the standardization of the methodology.

Technique's steps, that are considered in this work, are:

- 1) Definition of the acquisition protocol and choice of mathematical model to obtain liver perfusion parameters
- 2) Time Attenuation Curve fitting
- 3) Variability related to the operator
- 4) Variability related to the patient, the acquisition system and calibration of the CT.
- 5) Analysis of image processing technique, i.e. "ROI based approach" vs "pixel by pixel approach, i.e. quantitative value of perfusion map

In fact, Perfusion liver CT is spreading as a useful functional technique but no consensus has emerged about the better image acquisition protocol and the choice of image processing method to derive tumour liver perfusion parameters. Different mathematical models were applied to obtain quantitative perfusion parameters from CT perfusion scans but the commonly used model for describing the contrast enhancement perfusion signal is based on Fick principle, also called "Slope method".

Moreover, contrast enhancement and so perfusion values are influenced by patient's cardiac output and weight. However, a wide range of perfusion CT techniques have evolved and the various commercial implementations advocate different acquisition protocols and processing methods. In this manuscript we analyze different causes of variability related to perfusion CT exams in liver tumours analysis, testing new algorithms and giving guidelines to reduce the elements of uncertainty of image processing analysis in the characterization of HCC arterial hypervascularization.

Because some authors indicate that a surrogate functional measurement in Perfusion CT studies (as Standardized uptake value in PET studies) would be useful in characterization of tumour neoangiogenesis, we have developed an algorithm to calculate from region of interest and pixel-by-pixel analysis a SPV index. The significance of SPV index in characterization of arterial HCC vascularisation was also assessed. Such software would be directly analogous to SUV software currently implemented on PET system. In conclusion, although Perfusion CT present some limitations in the processing analysis, this techniques are becoming an important tool in medical research and in clinical practice.

The research activities, described in this thesis, have produced scientific results published on scientific journal or presented at national and international congresses. Below the list of all the publications is reported:

- Papers published on scientific journal:

- **M. D'Antò**, M. Cesarelli, F. Fiore, M. Romano, P. Bifulco, A. Vecchione. Sources of variability in the use of standardized perfusion value for HCC studies. Open Journal of Medical Imaging. 2012, 2, 33-40

- Abstract of papers presented at National and International congresses:

- **M. D'Antò** , M. Cesarelli , P. Bifulco , M. Romano , F.Fiore , V.Cerciello , T.Cerciello “Perfusion CT of the liver: slope method analysis”. Secondo Congresso nazionale di Bioingegneria, Torino 2010, Atti Pàtron editore. pp. 467-468
- **Michela D'Antò**, Mario Cesarelli, Paolo Bifulco, Maria Romano, Vincenzo Cerciello, Francesco, Fiore, Aldo Vecchione. “Study of different Time Attenuation Curve processing in Liver CT Perfusion”. 10th IEEE International Conference on Information Technology and Applications in Biomedicine Corfù, Greece, 2010, paper N. 101

- Presidente, M. Romano, R. D'Angelo, F. M. Ronza, M. Cesarelli, F. Fiore, **M. D'Antò**. “A new procedure to obtain Standardized Perfusion Value to assess HCC vascularization: early clinical experience” European Congress of Radiology, Vienna, 2011
- **M. D'Antò**, M. Cesarelli, P. Bifulco, M. Romano, R. D'Angelo, F. Fiore “Parametric mapping of the Standardized Perfusion Value in Hepatocellular Carcinoma”, European Congress of Radiology, Vienna, 2012
- F. Fiore, **M. D'Antò**, S.V. Setola, P. Bifulco, M. Romano, M. Cesarelli, “Cause di variabilità nell'applicazione dell'indice di perfusione Standardized Perfusion Value nei pazienti con HCC” 45 Congresso SIRM 2012, Torino
- **M. D'Antò**, F. Fiore, M. Romano, P. Bifulco, M. Cesarelli “Reliability of perfusion maps in HCC patients” GNB2012, June 26th-29th 2012, Rome, Italy

2. LIVER PERFUSION CT

This chapter presents the theory of Liver Perfusion CT technique. The physiological process of liver tumour vascularisation is described.

2.1 LIVER PHYSIOLOGY

The liver has a unique perfusion system with a dual blood supply. More than two-thirds of the blood supply comes from the low-pressure portal vein, and the rest comes from the high-pressure hepatic artery. The capillaries of the liver, called ‘sinusoid capillaries’, therefore contain a mixture of portal and arterial blood. The sinusoid capillary system is very dense, representing almost one third of the volume of the liver parenchyma. The endothelial cells that line the sinusoids are anatomically and biologically different from endothelial cells in other organs.

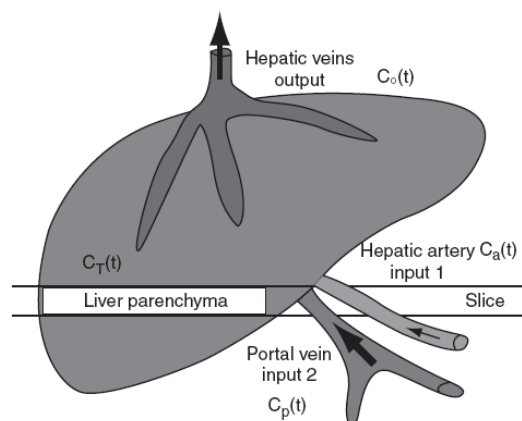


Figure 1: The liver is supplied more than two-thirds by the portal vein and less than a third by the hepatic artery. A transverse slice through the abdomen allows simultaneous measurement of the attenuation in regions of interest (ROIs) drawn in the portal vein, in the aorta, and in the liver tissue.

They lack a basement membrane and contain fenestrae, characteristics that facilitate the transport of nutrients and macromolecules between the sinusoids and the hepatic parenchyma. The hepatocytes

lining the sinusoids represent most of the volume of the liver parenchyma, and the interstitial space, called the 'space of Disse', is almost virtual, representing only 10% of the total liver volume. Specialized pericytes called stellate cells (or Ito cells) are located in the space of Disse and wrap around the walls of the hepatic sinusoids. Regulation of blood flow and vascular resistance in the hepatic microvasculature are intimately linked. Whereas in most organs the site of blood flow regulation occurs at arteriolar level, in the liver most of the blood flow enters at low pressure through the portal vein, and resistance changes occur in the sinusoid. Stellate cells play a role in the regulation and control of blood flow through the liver based on their anatomic location and contractile characteristics by modulating the sinusoidal caliber in response to several vasoactive endothelium derived mediators including nitric oxide (NO). The portal supply varies greatly during the day in relation to bowel activity, with large increases in the postprandial periods. The total hepatic blood supply, however, is finely tuned by the so-called 'hepatic arterial buffer response', which is the inverse response of the hepatic artery to changes in portal vein flow. These intrinsic regulatory mechanisms based on the local concentration of adenosine tend to maintain total hepatic blood flow at a constant level, allowing an increase in the arterial blood supply to compensate for a decrease in portal supply, and a decrease in arterial blood supply in cases of increased portal supply. It is important to note that, in contrast, variations in arterial blood supply cannot be compensated by variations in portal supply.

The specific dual perfusion of the liver makes it more difficult to analyze it with contrast-enhanced imaging than the perfusion of other tissues. The enhancement curve of the liver, after the injection of a bolus of contrast agent, is the combination of the enhancement due to the contrast agent flowing in the arterial blood and the contrast agent flowing in the portal blood. Whereas the molecules of contrast agent arrive quickly when they are delivered to the liver through the arterial route, they are delayed and diluted by the splanchnic circulation when they are delivered through the portal route.

Many strategies have been developed to take advantage by the portal lag to separate and quantify the arterial and portal hepatic perfusions. A comprehensive review of perfusion imaging of the liver has recently been published by Pandharipande et al [1].

2.2 BASIS OF PERFUSION CT

Perfusion CT technique typically requires a baseline image acquisition without contrast enhancement followed by a series of images acquired over time after an intravenous bolus of conventional contrast material. Because blood attenuates X-rays uniformly on the scale of the spatial resolution of a CT scanner, flowing blood cannot be differentiated from stationary blood. To measure tumour perfusion with CT, a contrast agent is injected intravenously, to 'label' the blood. Assuming that the injected contrast is uniformly mixed with blood, tracing blood through the tumour circulation is equivalent to tracking a bolus of contrast through the tumour. As such, we can make use of the extensive literature on tracer kinetics modelling in the measurement of CT tumour perfusion. Note that in this thesis we use the terms perfusion and blood flow interchangeably. Blood flow (F) can be defined as the volume flow rate of blood through the vasculature in a tumour. It is usually expressed in units of ml/min/100g or ml/min/100ml.

Also, in the diagnosis of tumour or the study of tumour biology, it is highly advantageous that besides perfusion we can measure additional functional parameters in the same study.

The fundamental processes underlying CT measurement of tumour perfusion and associated hemodynamic (functional) parameters are the transport by blood flow of an intravenously administered iodinated contrast agent to the tumour. With the current fast CT scanners tissue contrast concentration can be measured and traced over time at short intervals to allow detailed modelling of the distribution of contrast agent in tissue. In fact the resulting temporal changes in contrast enhancement, often displayed as time attenuation curves (TAC) (Fig. 2) are subsequently analyzed to quantify a range of parameters that reflect the functional status of the vascular system.

Compartmental models and linear systems based methods for contrast transport and exchange have been developed to quantify tumour blood flow, blood volume, mean transit time, and other parameters (see the following chapter for details).

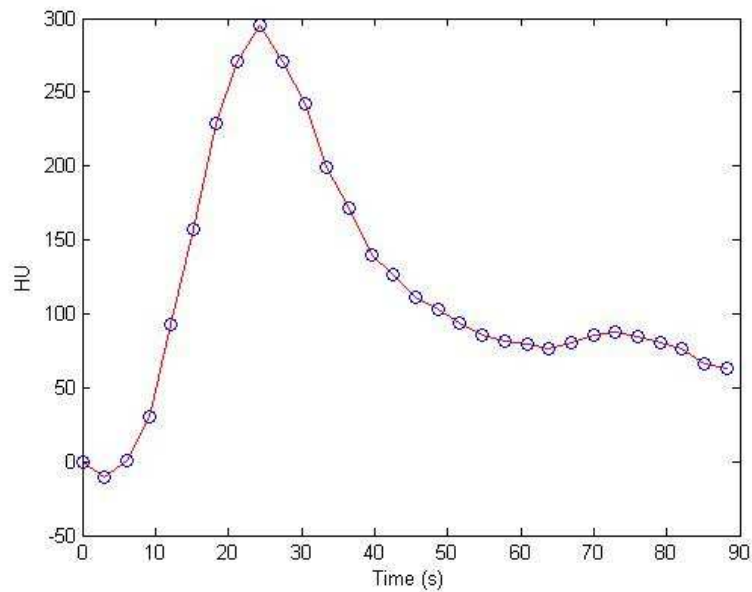


Figure 2: An example of Time attenuation curve (TAC). This curve has been obtained positioning a ROI (Region of interest) on aorta. Blue points represent means of HU values inside the ROI and were computed for each slice of the sequence (at different acquisition time) to compute a mean tumour-TAC.

2.3 PERFUSION CT ASSESSMENT OF HEPATOCELLULAR CARCINOMA (HCC)

Folkman and colleagues [2], in the 1960s, first proposed the dependence of sustained tumour growth on angiogenesis, a relationship that continues to be heavily explored today [3][4]. In patients with cirrhosis, a spectrum of nodules, including benign regenerative nodules, dysplastic nodules, and HCC, can form; differences in their respective blood supplies can assist in their detection and characterization [5][6][7][8]. Regenerative nodules, like normal liver parenchyma, continue to receive a majority of their blood supply from the portal vein, whereas the evolution from a low-grade dysplastic nodule to frank HCC is associated with a progression toward increasing arterial blood supply [5][6][7][8] (Fig 3).

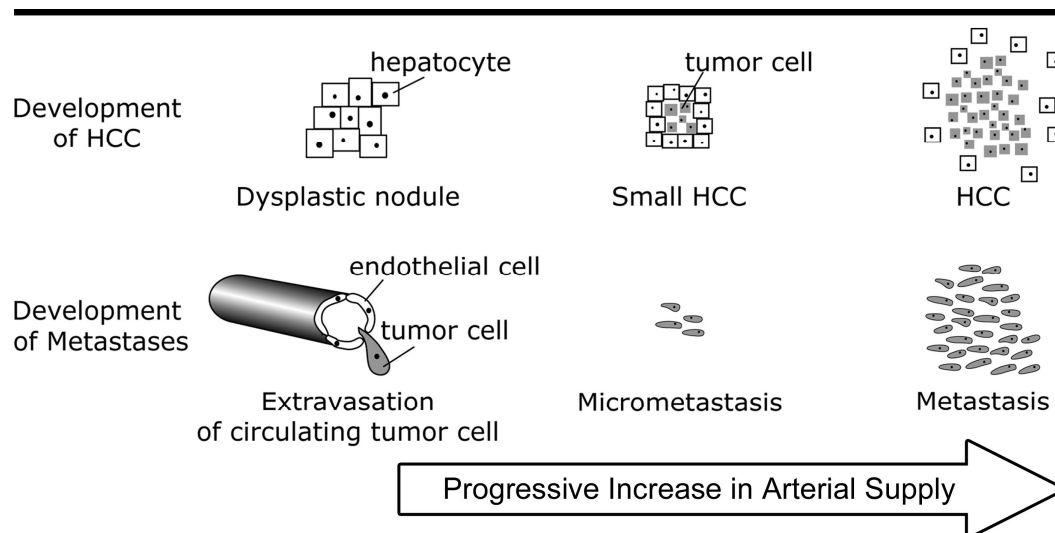


Figure 3: Diagram shows physiologic basis of perfusion imaging for tumor surveillance. Progressive increase in arterial versus portal venous supply is associated with both the evolution from a low-grade dysplastic nodule to frank HCC and the development of a metastasis from a circulating tumor cell.

During this evolution, sinusoidal endothelial cells are recruited to create an arteriolar network that gradually replaces normal sinusoidal architecture, and this process is known as “capillarization” [5]. At histological analysis, dysplastic nodules and HCC manifest neoarteriogenesis, which takes the appearance of unpaired or nontriadal arteries, that is, arteries not associated with portal vein branches [5][7][8]. Vascular endothelial growth factor expression, a marker of angiogenic activity, has been found to increase linearly and parallels the development of unpaired arteries [9]; it is negligible in regenerative nodules, moderate in dysplastic nodules, and strong in HCC [9]. Given this progression, serum vascular endothelial growth factor levels in patients with HCC have been explored as markers of tumor activity [10] and as predictors of postoperative tumour recurrence and survival [11].

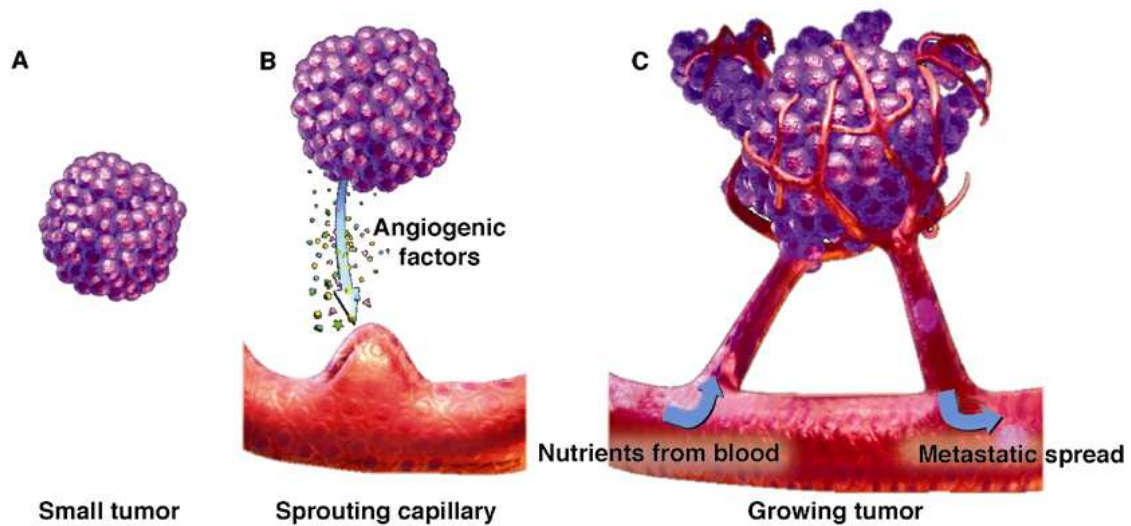


Figure 4: Neoangiogenesis process in tumour development

Perfusion CT studies are increasingly used in the HCC imaging. This aspect is facilitated by the current availability, on the market, of multislice spiral CT systems and commercial software packages and promoted by the diffusion, in routine clinical practice, of anti-angiogenic therapies. Neoplastic angiogenesis is in fact an important prognostic factor and a promising target for new treatments, of fundamental importance for monitoring tumour growth. Different techniques of image processing have been employed, in recent years, to obtain information about angiogenic characteristics of tumours in a non-invasive way. Among them, CT perfusion is advocated as a means to assess the grade of vascularisation in tumour tissue. This is supported by studies, which have reported a correlation between contrast enhancement parameters and histological measurements of angiogenesis [12,13]. CT perfusion is also employed to evaluate variations in perfusion parameters following regional treatments in loco or antiangiogenic drugs [14][15][16].

The clinical value of perfusion CT in the assessment of HCC and its correlated hypervascularization is confirmed by a lot of literature in this field. In the last two decade numerous studies have confirmed that perfusion CT is one of the best imaging acquisition technique to characterize HCC lesion [17][18][19].

Arterial hypervascularization is considered an essential aspect to evaluate the grade of aggressiveness of HCC tumour. In fact tumor HCC angiogenesis induce an increase of vascularisation in tumour which is reflected by an arterial blood flow increment in CT perfusion exams. In normal liver parenchyma arterial hepatic component is about 20 ml/min/100ml. Values greater than 40-50 ml/min/100ml are compatible with HCC lesion [20][21][22][23][24].

3. MATHEMATICAL MODELS FOR LIVER PERFUSION QUANTIFICATION WITH CT

Since perfusion CT has been introduced in clinical practice different mathematical model have been applied to TAC to obtain quantitative perfusion parameters. In this chapter the principles of these mathematical modelling for liver perfusion quantification are described.

3.1 SLOPE-RATIO METHODS

The basic model is very general and since the derivation of similar techniques by Fick in the 1870's, has been applied to tracers as diverse as dye and heat as well as CT contrast. Slope method is based on a compartmental analysis, often termed a black box analysis. The contrast material is modelled as entering an organ via an artery and rapidly distributing itself uniformly within the blood vessels and extra cellular space, and then, after a short interval, starting to leave the organ via a vein, see Figure 5.

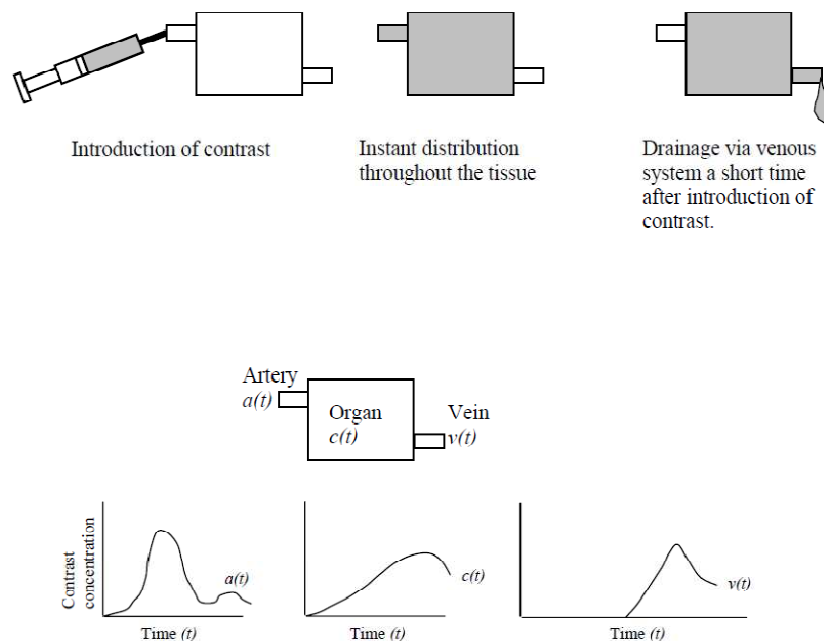


Figure 5: Black box model of flow and typical time attenuation curves (TAC) , where $a(t)$ is the concentration of contrast material in arterial blood showing a recirculation peak, $c(t)$ the concentration of contrast material in the tissue and $v(t)$ the contrast material concentration in the draining vein.

A simple approach of this sort can be used to model and calculate perfusion.

3.1.1 DRAINING VEIN ASSUMPTION METHOD

At any time t , let $a(t)$ be the arterial concentration of contrast agent, $v(t)$ be the venous concentration and $c(t)$ be the tissue concentration within a volume of tissue to be examined. Consider a volume of tissue, V , corresponding to a voxel and the flow into this volume as F . Then by definition, the perfusion P of the voxel is F/V . Consider the time interval $(t, t+\delta t)$. The amount of tracer arriving in the voxel is $F\delta t[a(t) - v(t)]$. This is the change in the amount of tracer in the voxel, i.e. the change in $[V c(t)]$.

Thus

$$1. \delta[c(t)V] = V\delta[c(t)] = F\delta t[a(t) - v(t)]$$

Going to the limit and integrating with respect to t :

$$2. P = \frac{F}{V} = \frac{c(t)}{\int_0^t a(t)dt - \int_0^t v(t)dt}$$

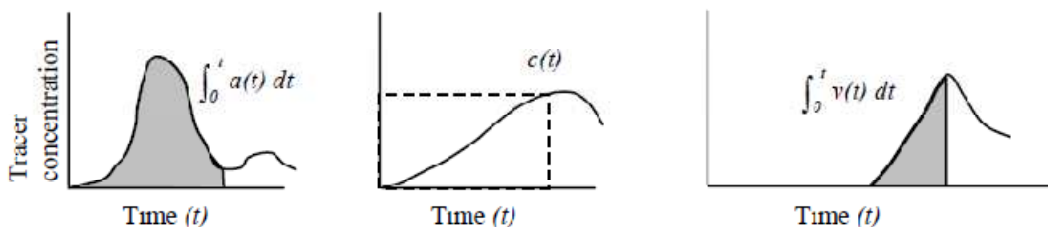


Figure 6: Draining vein assumption Perfusion can be expressed as tissue concentration at time t , $c(t)$, divided by difference between the area under arterial curve, $\int a(t)$, and the area under the venous curve, $\int v(t)$.

Thus if artery, venous and tissue concentrations are able to be determined, perfusion can be calculated, see Figure 6. This approach has been used with radioactive tracers using probes positioned over the organ and arterial and venous blood sampling. Unfortunately few imaging systems, including standard CT or MRI, can simultaneously measure input, output and parenchymal areas easily.

To determine perfusion we wish to sample the change of tracer concentration over a comparatively short period of time, so we require more rapid imaging. Rapid imaging is generally limited to a single section of the patient in which it is difficult to obtain an image of the organ, its artery and vein. Fast electronbeam CT scanners are an exception, as they can very quickly acquire a series of transaxial slices. They have been used to study perfusion, notably cardiac perfusion, using the formulation described above.

3.1.2 NO VENOUS OUTFLOW METHOD

A more realistic situation is imaging of arterial and tissue concentrations but not venous concentrations. If a bolus of tracer is given in a reasonably short time, we may assume that the venous outflow of tracer is negligible for a time less than the transit time of the tracer through the organ. Let this time be t_{ven} . Thus $v(t) = 0$ for $t < t_{ven}$, so that from equation 2:

$$3. P = \frac{c(t)}{\int_0^t a(t)dt} (t < t_{ven})$$

To minimize error this ratio is determined when the numerator and denominator are at their maximum. Let t_{max} be the time of peak parenchymal contrast concentration and as long as;

$$t_{max} < t_{ven}$$

$$4. P = \frac{c(t)_{max}}{\int_0^{t_{max}} a(t)dt}$$

If the time for the tracer to complete a loop of the entire vasculature system is less than the time to maximum concentration in tissue, the arterial concentration curve shows peaks due to re-circulation of the contrast material. The first pass phase of a contrast material is often modelled by a gamma variate fit to avoid the peaks due to re-circulation.

The arterial concentration is modelled using the gamma fit as

$$5. a(t) = k(t - t_0)^\alpha e^{-\frac{(t-t_0)}{\beta}}$$

Where $a(t)$ is the modelled increase in vascular contrast over baseline, t is the time, t_0 is the arrival time of the contrast at the vascular region of interest, see Figure 7.

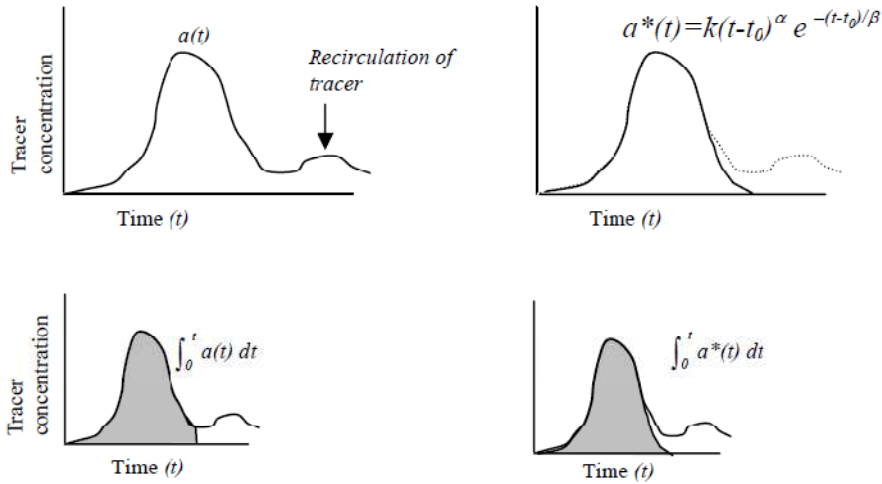


Figure 7: Arterial gamma variate fit to correct for recirculation. The arterial concentration curve, $a(t)$, is modelled by a gamma variate fit, $a^*(t)$, to limit the effect of the recirculation of the tracer on the area under the arterial curve.

When a gamma variate fit is applied to the arterial time concentration curve a model of first pass curve is produced $a^*(t)$. This modelled curve does not have the recirculation peaks. Thus the area under this curve approximates the total contrast delivered to the organ without errors due to recirculation.

Thus we can calculate:

$$6. \int_0^{\infty} a^*(t) dt$$

which is a measure of the area under the arterial curve if we had a tracer that did not undergo recirculation. The reason for doing this is to allow the denominator of Equation 4 to be independent of t_{ven} , the time of venous outflow appearance. There remains the assumption that the $c(t)_{max}$ occurs prior of the recirculation and it is thus unaffected by recirculation of contrast material.

Perfusion is then calculated as

$$7. P = \frac{c(t)_{max}}{\int_0^{\infty} a^*(t) dt}$$

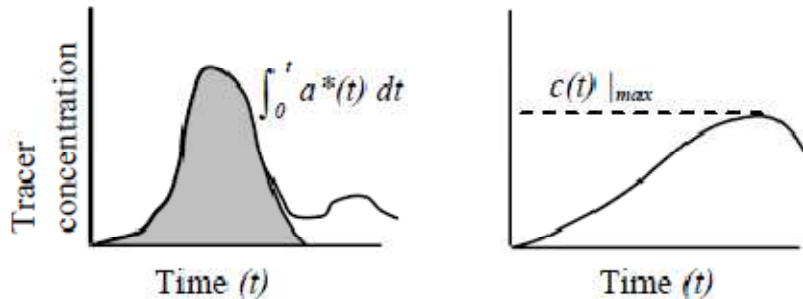


Figure 8: Arterial gamma variate area and maximal tissue enhancement.

Thus: Perfusion is the ratio of the maximal tissue enhancement to the area under the arterial time attenuation curve.

In literature, this relationship is variously referred to as the Sapirstein Principle, the Single Compartment Formulation or the Mullani-Gould formulation see Figure 8. This often underestimates higher values of perfusion with intravenous injection because the assumption of “no venous washout” is violated. Thus to apply this method we require that the time to peak of the tissue time-density curve (which is related to the width of the input bolus) is shorter than the minimum transit time of the system. The method can be applied to the abdomen using a time enhancement curve from an aortic region as an ‘input function.’ Note that this implies that we assume that there is no significant broadening or perturbation of the time enhancement curve between the aorta and the afferent arterioles. This is generally the case but the assumption would fail in the case of a stenosis between the aorta and the relevant afferent arterioles.

3.1.3 GRADIENT METHOD

A variation of this formulation for perfusion can be obtained if we differentiate equations 2 to 4, obtaining:

$$8. P = \frac{\frac{dc(t)}{dt}}{a(t)-v(t)}$$

from equation 2 and

$$9. P = \frac{\frac{dc(t)}{dt}}{a(t)} \quad (t < t_{ven})$$

from equation 3. Again minimizing the error by using the peak value of the denominator and numerator we use t_{max}^* the time of the peak 'gradient' of parenchymal enhancement where $t_{max}^* < t_{ven}$. we obtain:

$$10. P = \frac{\frac{dc(t)}{dt}_{max}}{a(t)_{max}}$$

$$11. \text{Perfusion} = \frac{\text{Peak Gradient of the Tissue Time Enhancement}}{\text{Peak Arterial Enhancement}}$$

This assumes there is minimal distortion of the vascular time enhancement curve in the passage from the imaged artery and the afferent arteriole, i.e. maxima are identical. Thus it is no longer necessary to perform a gamma fit of the arterial curve to obtain the area under the curve unaffected by re-circulation as only the peak value is required, see Figure 8.

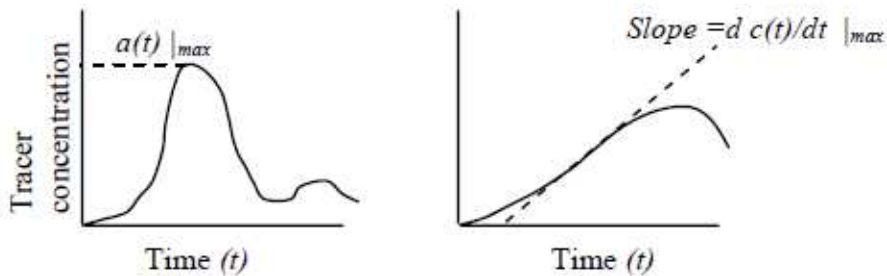


Figure 9: Peak arterial enhancement and peak gradient of tissue time enhancement curve

However, a gamma fit could still be applied to the arterial time enhancement data to reduce the underestimation of the peak enhancement due to the peak falling between two discrete sampling

points. This gradient approach was proposed by Peters et al.[25][26] for use in nuclear medicine studies and adopted for dynamic contrast-enhanced CT by Miles et al.[27][28][29]. The gradient method has the advantage that the tissue time-enhancement curve reaches its peak gradient well before its peak value. Thus the assumption that there is no venous outflow prior to time of the peak gradient rather than the longer time to peak is less likely to be violated. The use of early datum points to obtain a perfusion value also means that in imaging based modalities there is less likely to be patient movement due to breathing and may enable single breath hold imaging if the time to maximum slope for the organ of interest is sufficiently short. However this technique is innately more affected by noise as we are differentiating the data set. The gradient method, while having a shorter time required to determine the perfusion, may still have a time to maximum slope that is longer than the transit time in organs with a short transit time. This will lead to the breaking of the assumption of no venous outflow. The slope of the tissue enhancement curve and the time taken to reach the maximum slope are dependent on the bolus volume, the rate of injection and the patient's cardiac output.

The figure 10 presents a graphical representation of the three methods for perfusion determination based on compartmental analysis.

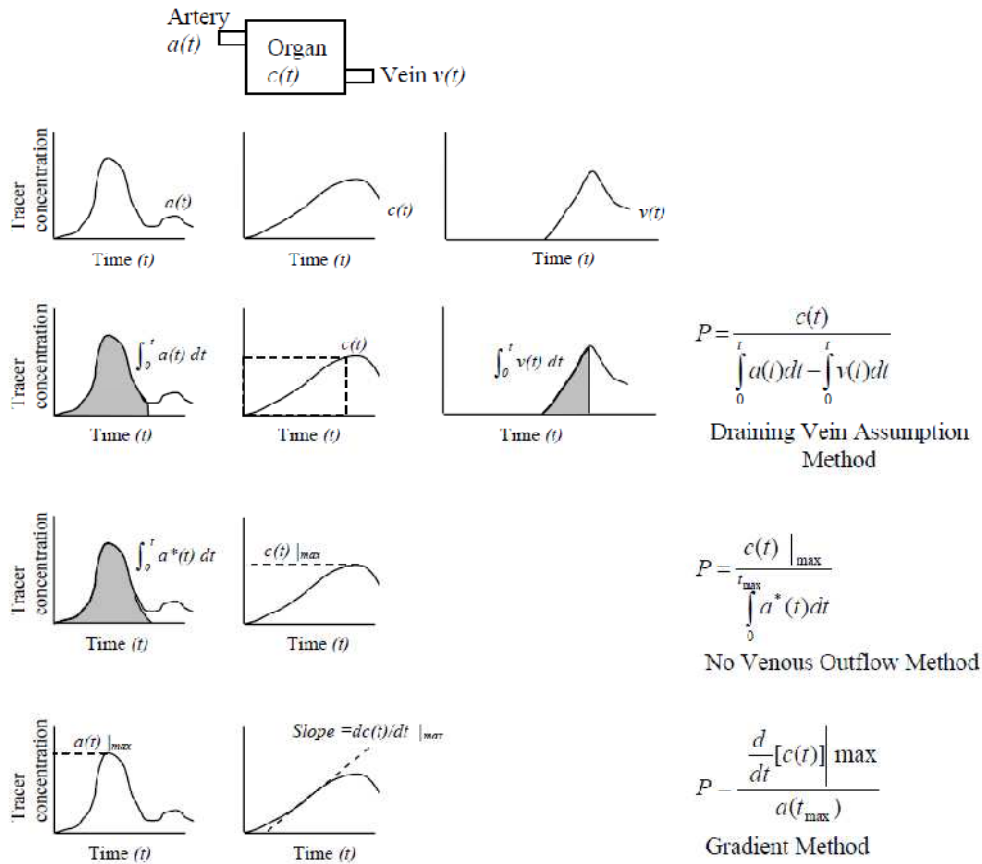


Figure 10: Schematic representation of compartmental model based perfusion calculation methods

3.2 MEASUREMENT OF BLOOD FLOW IN THE LIVER WITH “SLOPE METHOD”; PROBLEMS AND PROPOSED SOLUTIONS

There are several published studies that have considered perfusion in the liver. To date these have principally used the gradient method. The objective has been to attempt to quantify both arterial and portal perfusion. This requires to separate the effect of contrast arriving with the arterial blood from the portal blood arriving a short time later, and determining the magnitude of the two inputs.

3.2.1 TIME OF SPLENIC PEAK METHOD (ALSO CALLED “INDIRECT APPROACH”)

Miles et al. [28] described liver perfusion imaging using CT in 1993 by generating enhancement curves from regions of interest (ROIs) drawn over the liver, the aorta, and the spleen after a bolus injection of contrast agent.

Liver enhancement was resolved into arterial and portal venous components by assuming that maximum splenic enhancement marks the end of the early arterial phase and the beginning of the delayed portal venous phase of liver perfusion.

They assumed that prior to the time of the splenic peak there would have been no contrast from the spleen or other organs feeding the portal vein, thus up until this time, the liver could be considered to be supplied with only arterial contrast. This allows the arterial perfusion to be determined in the usual way:

$$\text{Perfusion} = \text{Maximum liver gradient} / \text{Maximum arterial enhancement}$$

The portal perfusion was calculated from the maximum slope of the remainder of the liver curve over the arterial enhancement, see Figure 11.

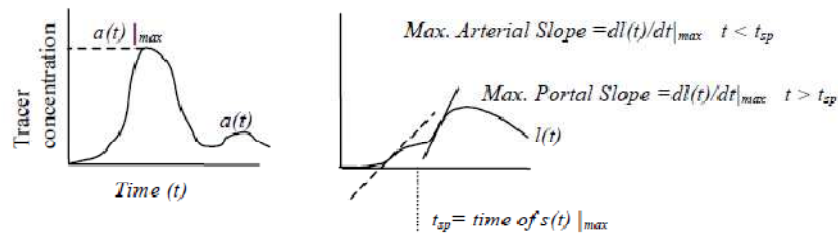


Figure 11: Arterial and portal perfusion phases of liver enhancement. a(t) Arterial enhancement. l(t) Liver enhancement curve showing maximal slopes contributing to arterial and portal perfusion. These phases are separated by the time of splenic peak enhancement.

This approach will lead to an underestimate of the portal perfusion for two reasons. The maximum enhancement of the portal blood supply will not be the same as that of the arterial. It will be lower due to dilution and broadening of the bolus in its transit through the spleen and other visceral organs. In addition the increase in enhancement due to the arrival of contrast in the portal blood will be masked by the reduction of contrast as the arterial blood flows out of the organ. The outflow of arterial contrast leads to an under estimate of the maximum slope due to portal contrast. Nonetheless this approach has shown clinical utility. However the method requires that the spleen be imaged in the transaxial slice.

The maximal slopes of the liver time–density curve in each phase were divided by the peak aortic enhancement to calculate both arterial and portal perfusion (BFa, BFp). The hepatic perfusion index (HPI), which is the ratio of the arterial perfusion to the total hepatic perfusion (HPI = arterial perfusion/ arterial + portal perfusion) was also calculated. HPI is also known as the ‘Hepatic Arterial Fraction’.

This technique is simple to implement and can be applied to any segment of the liver, as there is no need to include the portal vein or major portal vessel within the tissue imaged. However, the method underestimates portal hepatic flow for two reasons: first, the downwards slope of the last part of the arterial time–attenuation curve is superimposed on the upwards slope of the arriving portal curve; and second, the maximal slope of the portal venous phase of enhancement is divided by the peak aortic enhancement instead of the peak portal enhancement, which is flattened and diluted after flowing through the splanchnic system.

3.2.2 SCALED SPLEEN SUBTRACTION METHOD (ALSO CALLED “DIRECT” APPROACH)

To avoid these limitations, Blomley et al.[30] modified this approach by subtracting the arterial phase liver enhancement (modelled after splenic enhancement) from the liver enhancement curve to give a more ‘accurate’ portal time–attenuation curve. From this corrected curve, portal perfusion was calculated by dividing the slope of the rise in attenuation during the portal enhancement phase by peak portal venous enhancement itself.

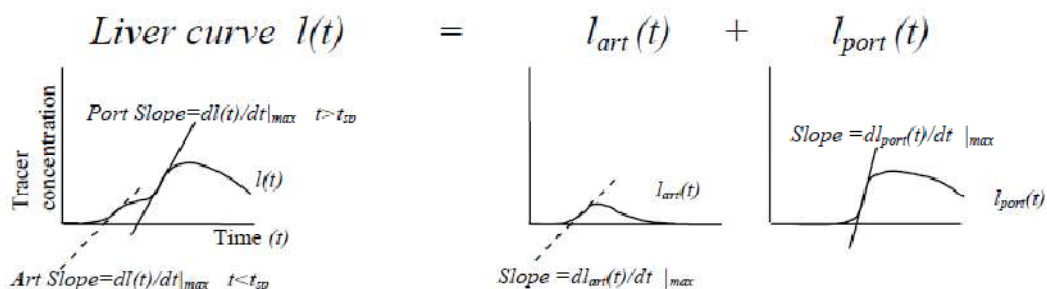


Figure 12: Liver enhancement curve as the sum of Arterial and Portal phases.

This ‘corrected approach’, however, has two main limitations.

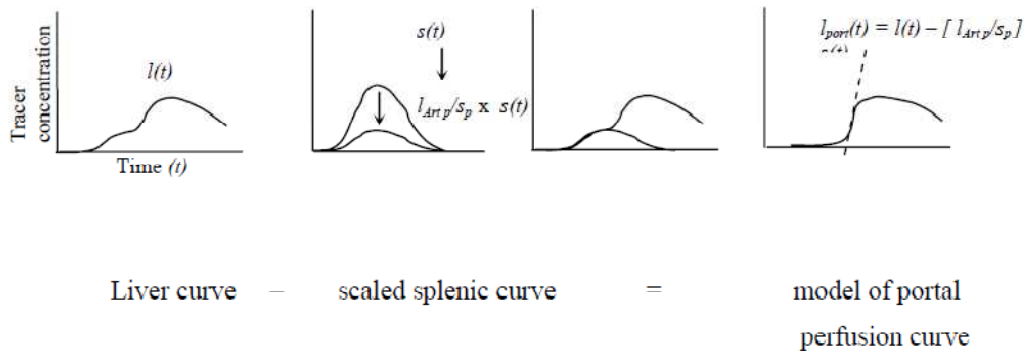


Figure 13: Portal enhancement as the difference of liver and scaled spleen.

First, it assumes that hepatic arterial and splenic enhancement curves are similar. Such similarity is unlikely in view of the unique microcirculation within the spleen, recognized as the mechanism underlying the transient splenic inhomogeneity seen during contrast-enhanced CT.

Second, the technique requires a set of slices containing both the portal vein and a part of the spleen to be able to draw ROIs and extract the enhancement curves.

3.2.3 SLOPE METHOD: “COMBINED APPROACH”

This method was introduced by White et al in 2007 and applied to liver perfusion MRI imaging. By literature analysis, it is possible to state that two main methods have been proposed for deriving perfusion measurements and HPI from CT time–density information. Both calculate arterial perfusion part by dividing the peak gradient in the liver during arterial phase by the peak enhancement of the aorta, but they differ in their approach to estimating portal perfusion. In the ‘‘indirect’’ approach portal component is calculated as the peak gradient in the liver during portal phase divided by the peak arterial enhancement.

$$12. BFp = \frac{\frac{dc(t)}{dt}_{port}}{a(t)_{max}}$$

Two refinements are made in the “direct” approach: the arterial component of hepatic uptake is removed before measuring portal uptake gradient (by subtracting a scaled enhancement curve from a purely arterial organ such as the spleen), and perfusion is estimated by dividing this corrected portal by peak enhancement measured in the portal vein.

Both techniques have been reported to show differences in perfusion between control subjects and patients with malignancy [30][28][31] but the “direct” method is more physiologically appropriate and, when applied to dynamic CT, provides portal perfusion values in closer agreement to those derived using other techniques [31]. This method is also less subject to errors arising from arterial washout and recirculation.

In “combined” method, portal perfusion is derived from gradient after subtraction of the arterial component from the liver curve (as in the direct method), but scaled to the enhancement of the aorta rather than that of the portal vein.

This approach makes the implicit assumption that a single blood concentration of contrast agent is applicable to both the arterial and portal perfusion, as in the “indirect” method used for dynamic CT measurements of the HPI [28]. However, since the relative hepatic and portal perfusion are both scaled to the peak of the aortic enhancement curve, this scaling factor appears in both the numerator and the denominator of the HPI and can be omitted entirely when only the HPI values are required. The “combined” method therefore lends itself to voxel-based HPI analyses because it removes the need for measurement of the aortic and portal venous concentrations of contrast agent. This enables the HPI analysis to be performed with minimal operator intervention, using rapid lower-resolution dynamic scans where the portal vein is difficult to isolate and where saturation effects in the aorta are hard to eliminate.

3.3 “DUAL INPUT ONE COMPARTMENT MODEL”

Van Beers and Materne have developed a compartmental model with a dual-input [32][33]

$$13. \frac{dC_l(t)}{dt} = k_{1a} C_a(t) + k_{1p} C_p(t) - k_2 C_l(t)$$

in which C_l , C_a , and C_p are the contrast agent concentrations measured over time respectively within the liver, hepatic artery, and portal vein derived from ROIs, and k_{1a} , k_{1p} , and k_2 are the arterial and portal venous inflow and liver outflow rate constants. By fitting measured $C_l(t)$, the constants k_{1a} , k_{1p} , and k_2 can be estimated, and can be used to calculate hepatic arterial and portal venous perfusion, mean transit time (MTT) of contrast agent through the liver, and contrast agent distribution volume within the liver (V_d). The distribution volume V_d of contrast agent is used instead of the hepatic blood volume, because the small-molecule contrast agent used in CT leaks freely and instantaneously across the sinusoid capillary wall, leading to a distribution volume that associates the hepatic blood volume and part of the extracellular Disse space.

This compartmental approach assumes that there is an instantaneous mixing of blood in the capillary compartment.

3.4 “DECONVOLUTION MODEL”

To avoid this assumption in the liver, where the capillary network is complex and the mean transit time long, Cuenod et al. [34] have developed a specific deconvolution technique. The deconvolution method considers that the time course of the concentration of contrast agent entering a tissue is modulated by a transfer function specific to the tissue. This transfer function can be computed from both the concentration–time curve of contrast agent entering the tissue (input) and the concentration–time curve of contrast in the tissue. From that transfer function, the perfusion parameters of the tissue can be calculated. The deconvolution strategy was introduced into functional CT by Axel in the 1980s [35]. The specificity of the liver, for this approach, comes from its dual vascular input. The method is described below.

Deconvolution allows the determination of the theoretical impulse response of the tissue, that is, the time course of concentration that an instantaneous input of contrast material (impulse input) would have yielded.

When the contrast agent enters the tissue as a function of time, $C_i(t)$, the time course of the concentration of contrast throughout the tissue depends both on the time course of a theoretical impulse input (instantaneous input) through the tissue, $h(t)$, and on the actual experimental time course of contrast input. The concentration–time curve at the venous outflow, $C_o(t)$, is the convolution of $C_i(t)$ by $h(t)$:

$$14. C_o(t) = C_i(t) * h(t)$$

However, since we cannot measure the time attenuation curve at the venous outflow of the tissue and can only measure the concentration–time curve of contrast into the tissue, we have to infer the venous outflow time attenuation curve from the tissue time attenuation curve. To do so, we use the notion of residue function. The integral of $h(t)$ is:

$$15. H(t) = \int_0^t h(\tau) d\tau$$

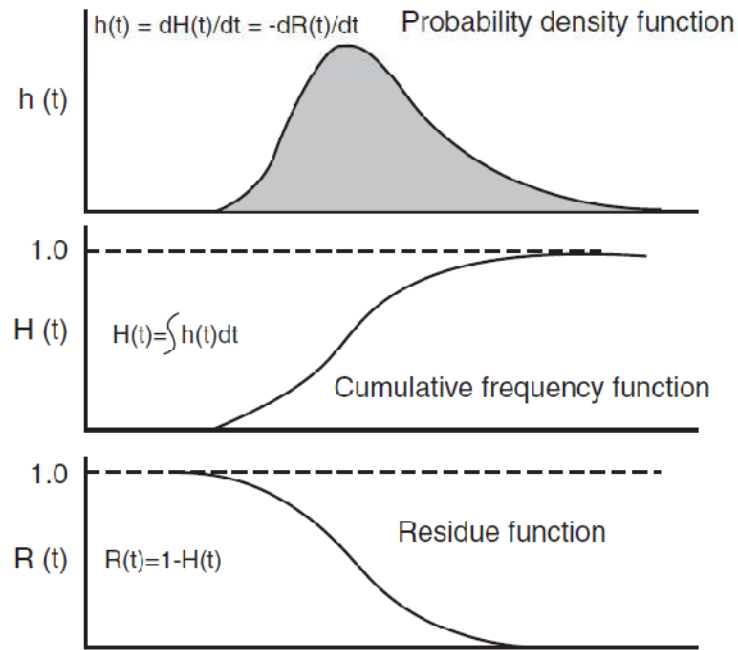


Figure 14: Relations between the residue function $R(t)$, the cumulative frequency function $H(t)$, and the probability density function $h(t)$. The contrast agent that progressively leaves the tissue accumulates outside the tissue. At the venous outlet the concentration of contrast agent rises progressively before decreasing to zero. The initial value of $R(0)$ is normalized to one, as well, therefore, as the final value of $H(t)$ and the area under the curve $h(t)$

where $H(t)$ is the fraction of an impulsive input which has already left the tissue by time t (Figure 14). It is called the cumulative frequency function. Its complementary function is called the residue function $R(t)$:

$$16. R(t) = 1 - H(t)$$

where $R(t)$ is the fraction of the impulsive input remaining within its distribution volume V_d in the tissue at time t . The concentration–time curve of a tracer remaining in its volume of distribution within the tissue $C_d(t)$ can be predicted for any type of input function, $C_i(t)$, as the convolution of $C_i(t)$ by $R(t)$:

$$17. C_d(t) = C_i(t) * R(t)$$

Because the distribution volume V_d of the tracer is within a larger volume of tissue V_t , the concentration of tracer within the tissue is:

$$18. C_t(t) = C_d(t)V_{dt}$$

where $V_{dt} = V_d/V_t$ is the fractional dilution volume of the molecule expressed as a percentage of the total volume of tissue V_t . The concentration of tracer in a voxel of tissue $C_t(t)$ is therefore the convolution of $C_i(t)$ by $R_t(t)$, the tissue transfer function ($R_t(t) = [V_{dt}R(t)]$):

$$19. C_t(t) = C_i(t) * R_t(t)$$

After contrast injection, a deconvolution process can allow the determination of $R_t(t)$, knowing the contrast variation of the tissue $C_t(t)$ and the input function $C_i(t)$. For finite time sampling steps of $\Delta t = T$, the convolution $C_t(t) = C_i(t)*R_t(t)$ can be approximated by the following sum:

$$20. C_t(nT) * R_t(nT) = T \sum_{k=0}^{n-1} C_i(nT - kT)R_t(kT)$$

The category of Weibull functions

$$21. g(t) = a \exp^{\frac{-t}{b^c}}$$

has been chosen to represent the tissue transfer function $R_t(t)$ because its shape is intermediate between a falling exponential function and a square function, resembling the supposed liver curve. A computer program is necessary to minimize the quadratic error between the measured tissue response $C_t(nT)$ at each time nT and the assumed response $C_t^*(nT)$ after convolution of the measured input $C_i(nT)$ at each time nT :

$$22. C_t^*(nT) = T \sum_{k=0}^{n-1} C_i(nT - kT) a \exp^{\frac{-kT}{b^c}}$$

The program yields the value of the three unknown factors a , b , and c , allowing the estimation of $R_t(t)$ (equation 19). Since $R_t(t) = V_d R(t)$ and $R(0) = 1$, then $V_d = R_t(0)$ and $R(t) = R_t(t)/R_t(0)$.

When $R(t)$ has been worked out, $h(t)$ can be obtained as its negative derivative

$$23. h(t) = -\frac{dR(t)}{dt}$$

and the output function $C_o(t)$ can be calculated.

The mean transit time (MTT) through the vascular bed can be calculated as the first moment (or the geometric mean) of the calculated $C_o(t)$:

$$24. MTT = \frac{\int_0^{\infty} t C_o(t) dt}{\int_0^{\infty} C_o(t) dt}$$

It can also be calculated as the first moment of the impulse response itself:

$$25. MTT = \frac{\int_0^{\infty} t h(t) dt}{\int_0^{\infty} h(t) dt}$$

and even more simply, knowing that,

$$26. \int_0^{\infty} h(t) dt = 1 \text{ as } MTT = \int_0^{\infty} t h(t) dt$$

The fractional distribution volume of the tracer V_{dt} , can be calculated as $R_i(0)$, the initial (maximal) value of $R_i(t)$. As expressed above, the fractional distribution volume of the contrast within the tissue, V_{dt} , is calculated as the initial (maximal) value of $R_i(t)$: $V_d = R_i(0)$.

The blood flow through a unit volume of tissue ($F_t = F/\text{volume of the organ}$) expressed as ml/min/100 ml is measured using the central volume theorem:

$$27. F_t = \frac{V_{dt}}{MTT}$$

Specifically in the liver, the dual blood supply has to be taken into account for the calculation. The respective balance between the arterial input $C_a(t)$ and venous portal input $C_p(t)$ of the liver is expressed as the hepatic perfusion index (HPI), which is the ratio of the arterial blood flow (BF_a) over the total hepatic blood flow BF_t :

$$28.HPI = \frac{F_a}{F_a+F_p}$$

In the liver, arterial and portal blood are mixed in the sinusoidal capillaries, and the tissue concentration–time curve in the liver (referred to as C_t) can be expressed as:

$$29.C_t(t) = [\alpha C_a(t) + (1 - \alpha)C_p(t)] * R_t(t)$$

Algorithms have therefore to minimize the quadratic error between the actual tissue response $C_t(nT)$ and the assumed response $C_t^*(nT)$ after convolution of the dual input: (Figure 15)

$$30.c_t^*(nT) = T \sum_{k=0}^{k=n-1} \left[\alpha C_a(nT - kT) + (1 - \alpha)C_p(nT - kT) a \exp^{-\left[\frac{kT}{b}\right]^c} \right]$$

The algorithm yields the value of the four unknown factors α , a, b, and c, allowing the estimation of $R_t(t)$ and $\alpha = HPI$. $R_t(t)$ allows the calculation of MTT, V_{dt} , and F_t , and HPI allows the calculation of $F_a = HPI \times F_t$, and $F_p = (1 - HPI) \times F_t$

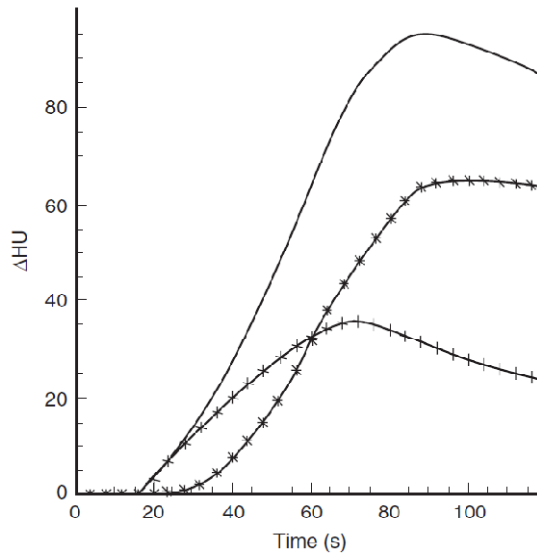


Figure 15: The time–enhancement curve of the liver, expressed as Hounsfield unit variation (HU) over time (continuous line), can be separated by the computer using the deconvolution model into the linear combination of the early and small enhancement curve of the arterial supply (crosses), and the late and strong enhancement curve of the portal supply (stars). The contrast enhancement is obtained by subtracting the mean baseline value from the values measured in the ROIs

<i>Name</i>	<i>Abbreviation</i>	<i>Definition</i>	<i>Unit</i>
Mean transit time	MTT	Mean time taken by molecules of contrast agent to flow through system	s
Liver distribution volume	LDV	Percentage of tissue volume in which the contrast agent distributes itself	% or ml/100 ml of tissue
Total hepatic blood flow	F_T	Total hepatic blood flow $F_T = F_A + F_P$	ml/min/ml of tissue
Arterial blood flow	BF_A	Hepatic blood flow of arterial origin	ml/min/ml of tissue
Portal blood flow	BF_P	Hepatic blood flow of portal origin	ml/min/ml of tissue
Hepatic perfusion index	HPI	Percentage of total blood flow of arterial origin $HPI = \frac{BF_A}{BF_A + BF_P}$	%

Table 1: The six main liver perfusion parameters that can be extracted with functional computed tomography (CT)

These parameters are obtained by drawing regions of interest (ROIs) on the aorta, the portal vein, and the liver parenchyma. The liver's ROI has to be drawn as large as possible, avoiding the large vessels. Then, the three ROIs are replicated by the computer on each image of the series to extract the CT attenuation numbers (expressed as Hounsfield units) over time. The time–attenuation curves derived from the aorta $C_a(t)$, the portal vein $C_p(t)$, and the liver $C_l(t)$ can then be used for calculation of the six hepatic perfusion parameters.

4. ANALYSIS OF SOURCES OF VARIABILITY IN PERFUSION CT STUDIES

In this chapter different causes of variability in perfusion CT parameters computation are debated and analyzed. First of all the problem of mathematical model adopted is introduced, due to its crucial role. Then, analysis were conducted to understand elements of variability related to processing of time attenuation curves once the model has been selected.

4.1 CHOICE OF MATHEMATICAL MODEL

The analysis of literature reveals that compartmental models (slope method and dual- input- one compartment model) are more used than deconvolution model to obtain liver perfusion parameters. Moreover they differ in terms of their theoretical assumptions and susceptibility to noise [12]. Slope method is based on the assumption that the bolus of contrast agent has to be retained within the organ of interest at the time of measurement which may result in underestimation of perfusion values in organs with rapid vascular transit or with large bolus injection. Whereas deconvolution model assumes that the shape of $R(t)$ is a plateau with a single exponential wash-out. Though this assumption works well for most of the organs, it might not be suitable for organs with complex circulatory pathways such as liver, for which it is preferable to use compartmental analysis. Deconvolution methods are appropriate for measuring lower levels of perfusion ($< 20\text{ml}/\text{min}/100\text{ml}$) as they are able to tolerate greater image noise due to inclusion of the complete time series of images in calculation. This is particularly beneficial for accurate measurement of lower perfusion values which are typically seen in tumours as consequence of treatment response. But then, the inclusion of all the acquired images, such as dual input one compartment model, for parameters calculation introduces possibilities of image misregistration due to motion of the patient. On the other hand, slope method effectively uses three images for perfusion measurement: the

baseline image and the image immediately before and after the time of maximal rate of contrast tissue enhancement and hence patient motion are rarely of significance.

Both types of modelling, however, are limited by the fact that the venous output is usually not measurable. Arterial Blood Flow, anyway, can always be calculated with slope method even if portal measurement is impossible (limitation of volume of coverage of CT system) or difficult (noisy TAC related to excessive patient's breathing). We remember that BF_a is the most important perfusion parameter to characterize HCC angiogenesis and its related to arterial hypervascularization. For this reason, as will be explained in the next chapter, BF_a computation is essential to obtain a Standardized Perfusion Value useful for studying HCC patients. The above considerations, as well as the results reported in this Section, support the idea that to obtain a standardized index helpful for analysis of all HCC patients, the use of the slope method is preferable (or even necessary).

In this research activity, deconvolution model algorithm is not analyzed and implemented. On the contrary, algorithms to implement slope method and dual input one compartment model are developed and tested. Moreover, to assess the dependence of perfusion parameter, in particular BF_a , from the mathematical method and to understand which is the best model in our specific research context, a comparison between maximum slope and dual-input one compartment model methods is made.

4.2 IMAGING STUDIES USED IN THIS THESIS

The results reported in this thesis were obtained from CT perfusion studies of twenty patients, with multiple or single hypervascular HCC lesions and without cardiac complications. Three of them were excluded from all the analysis because of poor quality in data images, this was due to patient's breathing, which, as known, represents an important reason of image misregistration in the CT perfusion of chest and abdomen. Therefore, seventeen patients (5 women and 12 men; age range, 52

- 83 years; mean, 69.3 years) were included in the study. The diagnosis of HCC tumour was achieved on the basis of AASLD (American Association for the Study of Liver Disease) criteria using established techniques (RM, MDTC and CEUS) or by means of liver biopsy for some of them. Weights and other relevant clinical information were collected for all patients. A target untreated lesion was selected on basal CTscan (without contrast). Then, perfusion CT study was performed for each patient. The project was approved by the scientific technical committee of the Hospital (National Cancer Institute “Pascale Foundation”, Naples, Italy) as part of an internal research project, with note DSC/1957 of 2009, all patients gave informed consent to undergo investigation.

Perfusion CT was performed by means of a commercially available scanner (Philips Brilliance 16 slices). The perfusion protocol comprised 30 scans (90 kVp, 250 mAs, 4×6 mm slice thickness, 1 second gantry rotation time, 3 s acquisition time), which were obtained in correspondence of tumour lesion. Each image has matrix dimensions equal to 512×512 .

CT perfusion study on localized HCC target lesion was performed after injection of 70 ml of iodinated contrast medium (Iomeron, 400 mg of iodine per milliliter) at a rate of 4 ml/s followed by 40 ml of saline solution, injected at a rate of 4 ml/s via an 18–20-gauge cannula in the antecubital vein. The following CT parameters were used to acquire dynamic data: 1-second gantry rotation time, 90 kV, 250 mAs and 6-mm reconstructed section thickness. Patients were instructed to breath as quietly as possible during the exam to reduce motion artifacts.

Our protocol is a compromise between patient’s health conditions and technical aspects related to the choice of compartmental analysis methods. The dynamic image acquisition, in fact, includes a first pass study until 60 second after bolus injection. This is in accordance with the idea of a unique compartment (intravascular and extravascular space are a unique “black box”) at the basis of slope method and dual input one compartment model.

For compartmental model, presence of image noise results in miscalculation of perfusion values hence a higher mAs value with lower image frequency is preferred with respect to deconvolution analysis.

Deconvolution method, being less sensitive to noise, allows the use of a lower tube current and allows scanning with higher temporal resolution [12]. The typical perfusion protocol for measurement of perfusion with deconvolution analysis is image acquisition for a total duration of 40- 60sec with 1 sec images every 1 second after injection of 40-50ml of contrast at a rate of 4-7 ml/sec with a tube current of 50-100mAs .

The typical image acquisition sequence for compartmental analysis in measurements of perfusion is for a total duration of 40-60sec with 1 sec images every 3-5 sec after injection of 40-50 ml of contrast at a rate of 7-10 ml/sec with a tube current of 100-250 mAs [12].

One of the important considerations for adequate assessment of perfusion of a tissue is the contrast medium bolus used for the intravenous injection. A short sharp bolus is essential for adequate perfusion assessment with compartment method and hence a small bolus of 40-50 ml is administered with a higher injection rate between 5 to 7 ml/sec.

Because our patients were often under chemotherapy treatment and didn't tolerate high injection rate to avoid complication, radiologists preferred to set 4 ml/sec as injection rate.

Due to linear relationship of iodine concentration and tissue enhancement a higher concentration of contrast media is preferred (370mg Iodine/ ml). To increase SNR our protocol provides a 400 mg Iodine/ml contrast media.

About the image processing, i.e. the algorithms developed, we exported patient's DICOM images and processed them using Matlab version 7.0.

4.3 IMAGE PROCESSING METHOD TO DERIVE PERFUSION PARAMETERS

4.3.1 PROCESSING OF TIME ATTENUATION CURVES

Time Attenuation Curve (TAC) represents the temporal evolution of attenuation coefficient corresponding to a voxel or a Region of Interest (ROI) and is proportional to the concentration of contrast agent in the region occupied by said voxel or ROI (in the following we'll call them respectively pixel TAC and ROI TAC). Hence, the temporal evolution of the gray value of a voxel/ROI is proportional to the temporal evolution of the average concentration of contrast agent within the voxel/ROI. ROI TAC can be obtained positioning ROI on the anatomical image acquired during perfusion study in a specific site (i.e. aorta, porta, liver, spleen) and calculating the mean HU value inside the ROI in all temporal slices acquired.

TAC are influenced by acquisition parameters such as the volume and the speed of the bolus of contrast material injected [12] and its temporal sampling is related to the temporal resolution of acquisition image process. A greater number of images results in more data points on TAC and therefore higher quality perfusion measurement although the radiation exposure increases.

Pixel and ROI TAC are used as input for algorithms based on mathematical model which compute functional parameters. So noise on this signal is responsible of inaccurate parameters computation and bias. Since ROI and pixel TAC exhibit high-frequency noise, some authors consider smoothing in the temporal or spatial dimension essential for a reliable analysis [36][37][38][39][40]. About pixel TAC, often they are also affected by photon noise. When generating TAC from very small regions or individual pixel, photon noise, in fact, becomes an important matter to take into account. Random variations in photon numbers cause variability in measured attenuation values and hence, errors in the calculated perfusion values [20]. However, at the best of our knowledge, no research work faces this matter in a detailed and specific way and, in fact, what is the best TAC processing is

still a debated topic. Of course, software implemented in commercially available instrumentation are generally not widely accessible.

Our experimental analysis of the curves has evidenced the problem of respiratory misregistration evidenced by the several peaks on the tumor TAC (see an example of our results reported in figure 16 and 17) in pixel and ROI analysis.

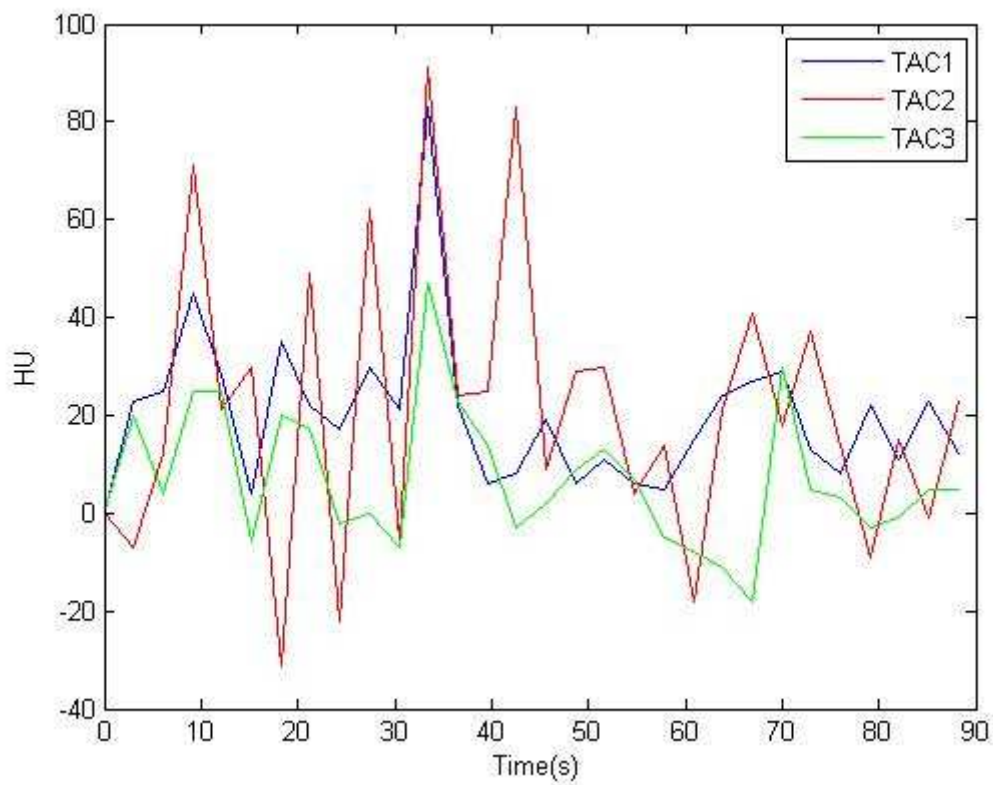


Figure 16: three pixel TAC represented with different colours

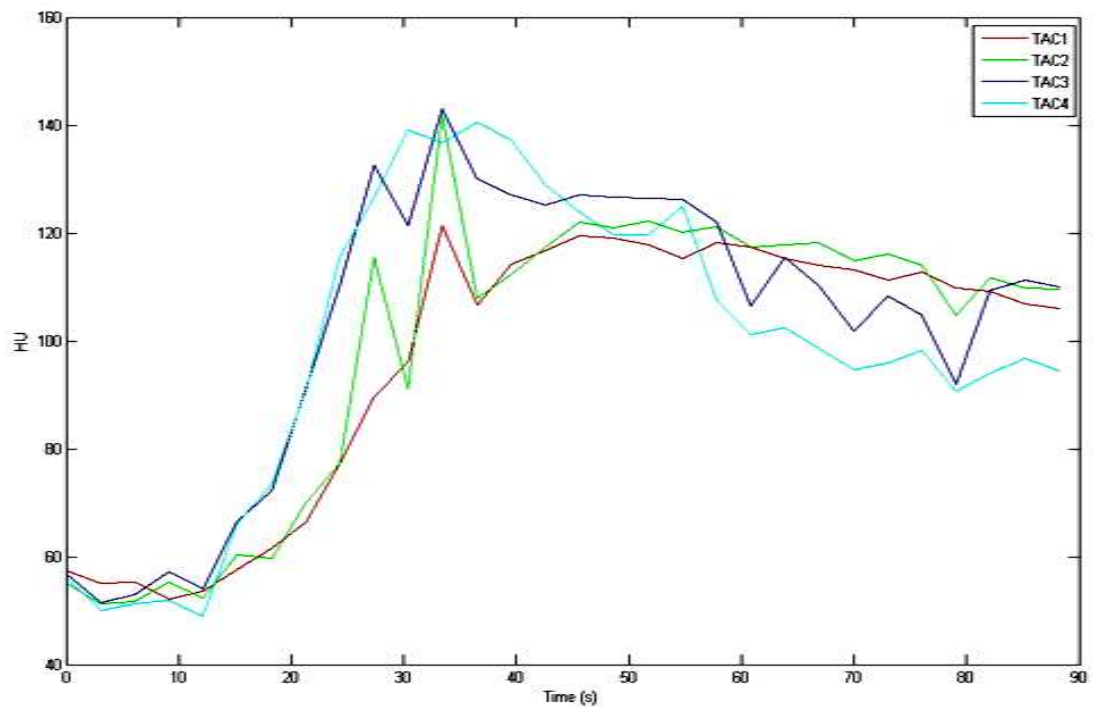


Figure 17: Four ROI TAC represented with different colours

Image registration technique and respiratory gating has been often proposed to solve the problem of respiratory misregistration. Image registration technique cannot always be applied because of the small volume of coverage of CT system (such as in this research project) and anyway this technique introduces an error that have to be quantified. Respiratory gating requires the use of advanced instrumentation not always available in Hospital (for example a simultaneous ECG recording or the employment of sensor to record patient movements). Some authors have proposed spatial and spatio-temporal filtering to reduce noise in perfusion CT images analyzing and proposing different algorithms to guarantee high fidelity of the time-attenuation curves and preserving edge and spatial resolution[38][39][40].

However, an inescapable problem in perfusion CT studies is that patients usually cannot hold their breath for 1 minute or longer, which is the duration of the imaging procedure. This inevitably leads

to motion artifacts that distort TAC in particular for CT exams in the abdomen. This leads to errors in perfusion values estimation and artifacts on parametric images [12].

Therefore, the original data of perfusion CT must be preprocessed before the mathematical calculation of perfusion parameters can be performed [36][37]. Data processing of original data points influences the shape of the curve and clearly the perfusion parameters.

4.3.2 SLOPE METHOD ANALYSIS: INFLUENCE OF TAC PROCESSING

One of the key points in the liver analysis by means of slope method is to assess the peak gradients of enhancement of the tumour TAC curves. However, imaging artifacts caused by patient respiration cause irregularities. Hence some method to attenuate these irregularities of the time density curve is required before the peak gradients can be assessed accurately.

Commercial software that implement slope method does not give specification about the processing algorithm implemented. Some of them automatically evaluate the maximum slope, others allow semiautomatic computation. Basama Perfusion software permits a manual selection of the maximum slope on the TAC in arterial and portal phase to calculate perfusion parameters [22][41]. The maximum slope can be defined as the greatest inclination of the straight line between the basal HU value and the maximum HU value on TAC. Some software automatically evaluate maximum slope, others allow manual selection on the TAC of the two points necessary to draw the straight line. However investigators have not provided details on the implementation of automatic maximum slope detection algorithms and this makes difficult results analysis and comparison. Particularly, processing for definition of starting and ending points of the straight line to identify the maximum slope have not been discussed. On the other side, manual selection introduces a significant variability due to the definition of the starting and the ending point on the TAC to obtain the straight line. In a preliminary analysis we have analyzed an important aspect that can affect the application of slope method and that, at the best of our knowledge, has not been yet investigated,

variability in estimation of BFa values obtained in semi-automated post-processing of CT perfusion images. To this aim, we estimated the BFa variability computed with a semiautomatic algorithm specifically developed based on a manual selection of the maximum slope of tumour TAC [42]. TAC can be calculated from circular ROI drawn over aorta, spleen and tumour. According to literature, BFa (in millimetres per minute per millimetre of tissue) was calculated by dividing the maximum slope of tumour TAC before the splenic peak by the peak aortic enhancement [20]. Our software allows a manual selection of the two points necessary to calculate the maximum slope. Because of the acquisition volume extended on four reconstructed slice, four TAC were obtained for each ROI. BFa parameter was calculated choosing the tumour TAC corresponding to the slice in which the tumour is more extended. To analyze BFa variability, related to slope evaluation, this parameter was evaluated in the same patient five times selecting any time on tumour TAC the two points necessary to obtain the maximum slope. BFa for the target lesion was calculated using the developed software five times in the same patient by the same radiologist to assess intra-observer processing variability. BFa values calculated with our algorithm were consistent with BFa HCC values reported in literature [43]. The mean values and the range for each patient are reported in table 2

	Patient 1	Patient 2	Patient 3
BFa values (ml/min/100ml)	0.42	0.41	0.76
	0.36	0.47	0.56
	0.52	0.35	0.63
	0.37	0.45	0.56
	0.48	0.52	0.74
Mean	0.43	0.44	0.65
Range	0.36 – 0.52	0.41 – 0.52	0.56 – 0.76

Table 2: BFa values computed in the three patients with a semiautomatic algorithm

The variability in BFa values is due to the manual selection of the two points necessary to calculate the maximum slope of the tumour TAC. However, when perfusion CT is used to monitor the effects of anti-angiogenesis drug therapy (to evaluate vascularisation tumour response), the reproducibility of the technique must be such that the difference between repeated measurements is small relative to the magnitude of the therapeutic change in perfusion. For this reason reproducibility of processing of CT perfusion data is a problem widely debated that limit the clinical application of this functional image technique. There are a lot of elements that influence reproducibility of perfusion CT software, independently from the mathematical methods, such as ROI input selection [44]. We have investigated the BFa intra-observer reproducibility linked to semi-automated application of the slope method. Obtained results highlighted the necessity to standardise the selection of starting and ending points in maximum slope assessment. Besides, the analysis of the curves has evidenced the problem of respiratory misregistration evidenced by the several peaks on the tumour TAC .

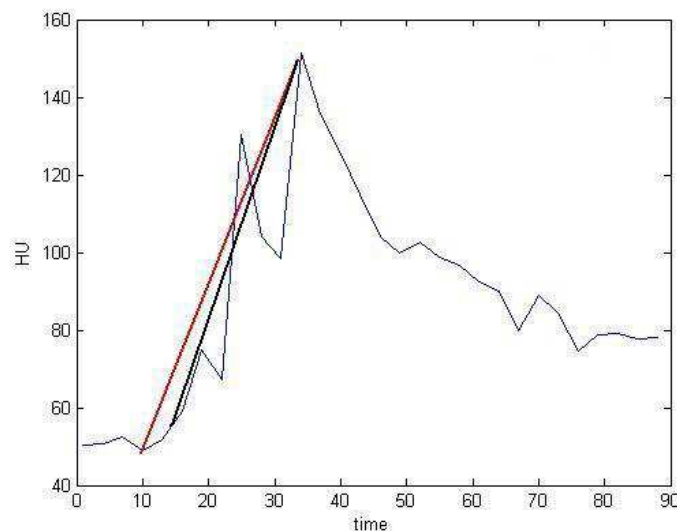


Figure 18: Peaks on TAC. The red and black lines represent two input selection from the operator on the same TAC

Peaks on tumour TAC almost certainly make difficult automatic detection of the maximum slope. The manual selection of the maximum slope, although introduces variability, seems to be robust to

the effect of respiratory misregistration because only one point, basal HU value, is operator dependent; in fact, the maximum value is undoubtedly identified.

Anyway intra-observer BFa variability in the selection of starting and ending point can be eliminated if, once the tumour ROI is selected, an automatic algorithm calculates the maximum slope of TAC curve. Therefore, these preliminary results revealed that new algorithms for an automatic selection of the maximum slope have to be investigated.

Moreover, in the preliminary approach the problem of TAC fitting has not been considered, analyzing only the problem of slope computation by manual selection of the line between minimum and maximum points. It's clear that processing of TAC can facilitate automatic algorithms for slope computation.

Therefore, successively, algorithms for an automatic selection of the maximum slope and the effects of different TAC processing techniques on BFa automatic computation have been investigated.

Some authors have studied the problem of TAC processing in slope method automatic implementation. Anyway we underline that no specification were declared about algorithms employed. Bader et al [36] pointed out that irregularity of the ROI TAC by motion artifacts caused an increase in the maximum slope of the curves and also represents a cause of perfusion liver parameter variability. In particular, they concluded that applying slope method to liver, motion artifacts and the type of data processing influence the assessment of the arterial, portal venous and total hepatic perfusion but do not influence measurement of HPI. They compare perfusion values obtained with a fitting procedure (with a gamma fitting) and a smoothing with use of weighted means algorithm.

Since our preliminary results on the group of three patients have showed that variability in slope selection can be reduced with an automatic algorithm, our idea was to test, according to Bader, the

effect of different automatic processing on TAC applying slope method [45]. We would have automatic but reliable algorithms which recognize effectively TAC slope.

As first step, to this particular aim, we proposed a new algorithm to remove outlier points related to breathing on TAC before the fitting procedure. Then we evaluated the effects of two fitting procedures applied to tumour TAC: gamma fitting, as suggested by literature [46], and smoothing spline interpolation. This two automatic procedures were compared with semiautomatic procedure (manual selection as proposed by Basama). The slope of the line that minimizes the mean square error was considered as the maximum slope in the selected interval. BFa was calculated in the same patient with these three different data processing.

The comparison of different TAC processing demonstrated that also applying the same mathematical model (slope method in our case) perfusion parameter computation is related to the employed data processing technique. Results about this aspect were obtained applying tested algorithms to image of eight patients (six males and two females; mean age, 66 years; age range, 52-76).

About data analysis on the axial image displayed by the software, a circular region of interest (ROI) was drawn around the liver tumour taking care to maintain the ROI within the boundaries of the mass. A further ROI was drawn around the aorta. Bfa was obtained from automated processing of the aorta and tumour TAC using the previously described method. Irregular points (i.e. peaks on TAC) are caused by reproducing a fixed ROI on the temporal images of the same anatomical level. Because of respiratory misregistration in z direction and x-y plane the selected ROI can include in the others temporal slices (of the same anatomical region) not only the tumour tissue but also air, bone or normal liver parenchyma. TAC unreliable data points were excluded with an algorithm that eliminates the points in which the first derivate is negative or equal to zero. Negative or zero slopes, until the maximum enhancement of the TAC is reached, are not consistent with our model. This is in accordance to the physiological assumption of an increase of contrast in the tumour that

corresponds to a continuous increment of HU signal (until the maximum enhancement of the TAC is reached) [12].

After this processing, the TAC of all patients were processed with two methods: a gamma fitting and a smoothing spline interpolation.

The gamma variate function is expressed as [46]:

$$31. y(t) = K(t - t_0)^\alpha \exp \frac{-(t-t_0)}{\beta}$$

where K, α and β are fitting parameters.

The gamma variate function has been often used to describe the dispersion of a bolus as it passes through a series of compartments [46]. For this reason, it is frequently chosen to fit first-pass data in perfusion studies. Although the gamma variate is an appropriate function to model these situations, it has several undesirable mathematical properties. Changes in the K, α and β parameters affect not only the rise and fall times of the function, but also the location and magnitude of the function maximum. This makes difficult to anticipate how the function will be altered by varying the parameters [46].

The smoothing spline is a method of smoothing (fitting a smooth curve from a set of noisy observations) using a spline function. The smoothing spline estimates the function μ (over the class of twice differentiable functions) that minimize the following equation:

$$32. \sum_{i=1}^n (Y_i - \mu(x_i))^2 + p \int \mu''(x)^2 dx$$

where p is a smoothing parameter, controlling the tradeoff between fidelity to the data and roughness of the function estimate [47]. The fitting procedure was obtained using the "csaps" MatLab function, where values csaps (x,y,p) return the values of the cubic smoothing spline for the given data (x,y) and depending on the smoothing parameter p from 0 to 1. In this study, p was the

default value chosen by csaps function. This choice is justified by the goodness of visual inspection of the results in all patients. Spline interpolation doesn't make any assumption about the shape of the TAC and represents a smoothing procedure that preserves the original shape of tumor liver pattern [48] [49] reducing undesirable irregularities on the rise of the curve.

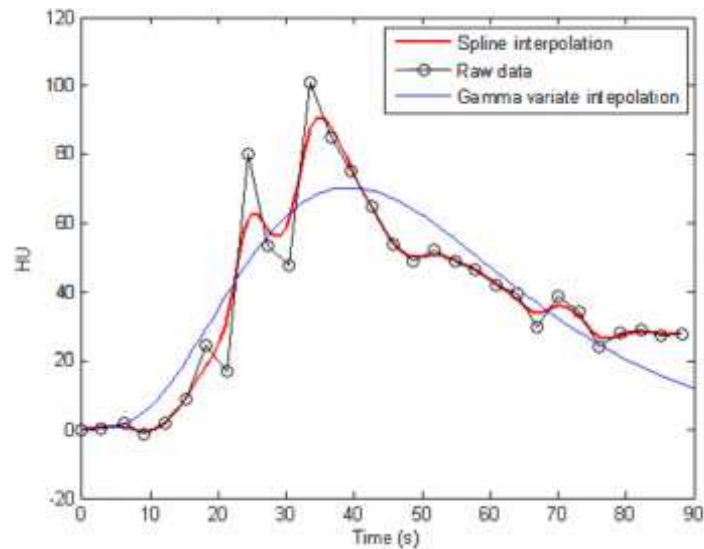


Figure 19: Results of different processing on the same raw TAC

Automatic evaluation of maximum slope, by means of first derivative computation, was implemented over the fitted curves and BFa value was calculated automatically dividing maximum slope by maximum enhancement value over aorta TAC. BFa was also evaluated for each patient allowing manual selection on the raw, original TAC (no fitted) of two points required to identify the maximum slope of the tumor TAC. The slope of the least squares line of the data points (within the selected interval on TAC) can be assumed as the maximum slope (green line plotted on Fig. 20).

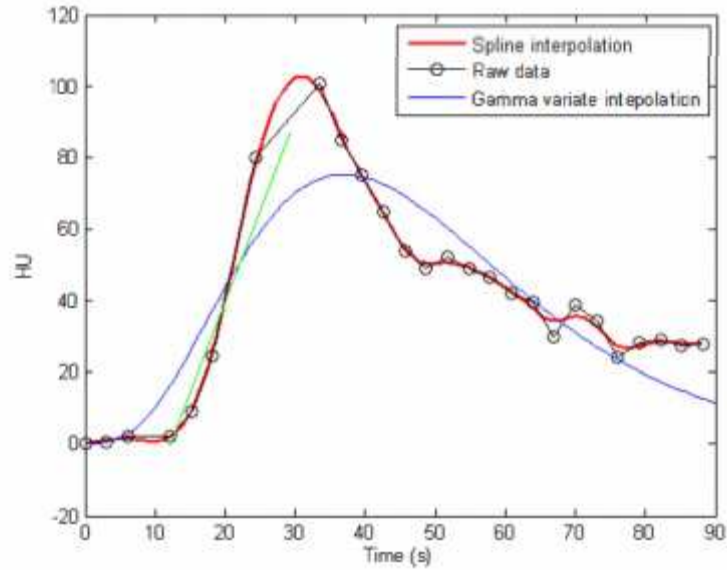


Figure 20: green line represent the maximum slope selected on the TAC

The results obtained showed that TAC are corrupted by respiration artifacts, in accordance with most recent studies [12] [36][49][50].

Irregular points are caused by positioning a fixed ROI on image. In the figures 19 and 20 an example of the effect of the first step of the proposed algorithm is shown. In Figure 19, the black dotted line (original data point) is affected by slope variation. In Figure 20, the black dotted line is monotonically increasing. The correction algorithm has removed points with zero or negative derivate.

Once tumour TAC were corrected, gamma and spline fitting were computed. Gamma fitting wasn't calculated in five patients because the data points obtained are not coherent with gamma variate approximation and with chosen parameters. In fact, gamma curve has a mono-exponential upslope and our study showed that is not suitable to represent the pattern of hepatic tumor enhancement. Spline smoothing interpolation, on the contrary, attenuates in all patients undesirable irregularities following the basic shape of tumor TAC (see Fig 20) [45]

The BFa values obtained with the different TAC processing methods are displayed in Table 3

	BFa (spline fitting)	BFa (gamma fitting)	BFa (no fitting with manual selection)
Patient 1	115.4	-	54.2
Patient 2	120.2	62.4	98.7
Patient 3	119.6	39.3	76.6
Patient 4	85.0	-	43.1
Patient 5	94.6	37.9	52.0
Patient 6	63.1	-	34.3
Patient 7	114.7	-	54.8
Patient 8	80.0	-	51.6

Table 3: BFa values obtained with the different TAC processing in eight patient

BFa computed from spline smoothing TAC interpolation were greater than those obtained with the other two data processing methods and are more consistent with BFa values reported in literature in HCC patient [43]. In fact, gamma fitting procedure causes an underestimation of BFa values because the end data points of TAC are not well approximated. This causes a flattening of the curve slope of the curve. BFa computed from manual selection were in all patients greater than values obtained with gamma fitted TAC. However, the estimation of maximum slope, after manual selection of start and end points, introduces a further element of variability [42].

In conclusion, we can state that fitting procedure and automatic detection of the maximum slope reduces the variability in assessment of perfusion parameters due to operator. Moreover, both spline interpolation and gamma fitting procedure are positively influenced by our correction algorithm. In particular, spline interpolation on corrected data points shows a single up-slope until the maximum enhancement is reached.

However, spline interpolation presented some technical difficulties, for example the automatic choice of smoothing factor – p value – is particularly difficult in noisy TAC, such as some of those derived from images acquired in clinical environments during daily practice. Hence, according to literature, we have considered interesting for research purposes considering also a moving average (MA - with five coefficient) still in comparison with manual selection of the maximum TAC slope.

When applying the two procedure of fitting (spline and MA filter), the TAC slope is obtained with a liner fitting of three data points relative to the maximum increment [51].

Since there are not certain guidelines in literature, BFa obtained with manual selection is here considered the reference.

The results of the comparison are reported in the following table 4.

Patient	BF_a , manual (ml/min/100ml) GRUPPO 1	BF_a , spline interpolation (ml/min/100ml) GRUPPO 2	BF_a , MA filter (ml/min/100ml) GRUPPO 3
1	80.22	127.5100	84.1100
2	77.3300	180.7700	71.7800
3	69.1200	125.3800	70.8600
4	84.1200	149.1400	85.1000
5	75.3300	113.8700	70.5900
6	79.5600	102.5200	77.7300
7	68.3300	117.2900	86.0100
8	120.4600	159.5900	104.5300
9	108.2000	130.2500	99.4300
10	65.5000	103.7700	64.3300
11	84.2300	100.1200	90.3300
12	55.2200	74.6600	49.4700
13	65.6900	167.5600	89.3400
14	49.0900	84.8000	56.9500
15	88.4300	120.1500	86.0500
16	78.2300	102.4100	80.2200
17	81.2300	129.6200	85.1300

Table 4: BFa values computed with different TAC processing. The nonparametric Mann-Whitney U test confirm that results from group one and three belong from the same population (statistical significance level of 5%)

The nonparametric Mann-Whitney U test was used to compare perfusion parameter (BFa) between the three groups. Null hypothesis is accepted only for group 1 and 3 with a statistical significance level of 5%.

The results obtained on a larger group of patients confirm that a moving average with fitting of three data point with maximum increment to compute the slope, represent an automatic and reliable method to obtain BFa with slope method.

4.4 COMPARISON OF MAXIMUM SLOPE METHOD AND DUAL-INPUT- ONE-COMPARTMENT-MODEL

The first study about the accord of perfusion CT parameters related to two commercially available perfusion computed tomographic (CT) software packages demonstrated that there was disagreement between mathematical model used to estimate tumour vascularity, which indicated the measurement techniques were not directly interchangeable [52]. Although many researchers have stressed the clinical usefulness of perfusion CT technique the standardization of analytical method, i.e. definition of the best mathematical model to compute hepatic perfusion parameter, is still matter of debate [53][54][55]. Kanda et al [53], comparing hepatic parameter obtained with maximum slope method (MS), dual input one compartment model (DOCM), and deconvolution method (DM), conclude that these three analytical method are not interchangeable. DOCM and DM are less susceptible to extra hepatic system factor, i.e. age , sex, cardiovascular risk, arrival time, transit time and liver dysfunction or hepatitis. A correlation coefficient of 0,455 ($p < 0,0001$) was calculated to study the agreement between MS and DOCM. Miyazaki et al [54] reported results about a simulation study to compare maximum slope and DOCM concluding that MS cause a underestimation of about 60% with respect to DOCM in BFa computation. In another work the same author [55] conclude that with venous injection BFa determined by the MS method was lower than that obtained by the DOCM method ($p < 0,05$).

No author have analyzed the susceptibility of this two methods to noise. So the purpose of our analysis was to study the effect of noise in BFa computation comparing MS (maximum slope) and DOCM (Dual input one compartment model) by simulations.

First, we generated $Cl(t)$ according to DOCM formula setting defined values for $K1a$, $K1p$ and $K2$ (in particular $K1a$ value was set to obtain a corresponding BFa values of 113,4). $Ca(t)$ and $Cp(t)$ were obtained from images acquired in a clinical perfusion CT study. In this study τ_a and τ_p were assumed to be zero for simplicity [54].

Furthermore, to investigate the effect of statistical noise, we added Gaussian noise to the TAC to generate signal to noise ratios (SNRs) of 20, 26 and 30. The SNR was given by the standard deviation of the power of noise free TAC divided by the standard deviation of the noise generated from normally distributed random numbers with zero mean and unit variance. Simulation were performed 10 times for each condition and the mean ad SD of the estimated BFa were calculated.

Results are reported in the following table 5:

		Veffsig/Veffn=20 SNR=26	Veffsig/Veffn =10 SNR=20	Veffsig/Veffn=30 SNR=30
BFa (ml/min/100ml)	MS	108,4±11,7	145,1±25,1	98,7±11,3
	DOCM	130,2±12,7	113,9±17,0	131,0±10,5

Table 5: Bfa values evaluated by MS and DOCM analysis. Results are reported in term of mean and standard deviation of ten simulation for each SNR conditions. Know value of BFa is 113,4.

Comparison between hepatic perfusion parameters evaluated with the two analytical methods were performed using Wilcoxon-Mann-Whitney test. $P < 0,05$ was considered significant. BFa determinate by MS method was lower than that determinate by the DOCM for higher values of SNR (26 and 30). When the noise is prevalent (SNR=20) slope method algorithm fail and give an

increment of BFa values. On the contrary mean value obtained with DOCM have the minor percentage change from the know BFa value. Our results suggest that our maximum slope algorithm give bad results in condition of low SNR (percentage change from the know BFa value is 21%). Anyway for other values of SNR (26 and 30) according to literature slope method underestimate BFa values with respect to DOCM method [54][55].

5. SPV INDEX IN CHARACTERIZATION OF ARTERIAL HCC HYPERVASCULARIZATION

Primitive liver tumour (HCC) diagnosis, assessment and staging are critical because PET (Positron emission tomography), that represent the gold standard functional technique, is not a useful tool in the diagnosis and follow up because HCC tumour are not characterized by an increment of glucose. So, perfusion CT studies in HCC patients are increasingly advocated as a means to assess the grade of vascularization to evaluate variations in perfusion parameters following locoregional treatments or antiangiogenic drugs.

One of the specific aim at the start of PhD candidature was to formulate a standardized index, such as SUV in PET studies, to characterize HCC Hypervascularization. In this Chapter we describe the theory about the SPV index in HCC and analyze the methodology and the causes of variability that have to be considered before that a reliable use in clinical practice is possible.

5.1 STANDARDIZED PERFUSION VALUE: HISTORICAL BACKGROUND

SPV index was introduced and applied to lung tumour vascularisation by Miles [56]. This author underline for the first time that perfusion parameter are largely unaffected by dose, patient weight, and cardiac output and that a dedicated image acquisition and relatively complex numeric analysis are required.

SPV index is defined as

$$33.SP\dot{V} = \frac{P_t}{P_{wb}}$$

where P_t is tumour perfusion and P_{wb} is mean whole body perfusion. P_{wb} is defined as Cardiac Output (CO) divided by patient's body weight (W). Cardiac output can be evaluated from perfusion CT images and defined as dose of contrast (D) divided by area under aortic curve (AUC).

The dose of contrast is calculated as below illustrated:

$$34. D = \text{volume of contrast (ml)} \times \text{contrast concentration} \left(\frac{\text{mg}}{\text{ml}} \right) \times K \text{ factor} \left(\frac{\text{HU}}{\frac{\text{mg}}{\text{ml}}} \right)$$

where K factor represent the calibration factor, i.e. the sensitive of CT system to iodine concentration.

The SPV is conceptually similar in its derivation to the SUV used to quantify FDG uptake at PET. The SUV is used to compare FDG uptake in the tissue of interest with the average uptake throughout the body. Likewise, the SPV is used to compare tissue perfusion with average whole-body perfusion. The results obtained by Miles showed good correlation between SPV and SUV in patients with lung tumour.

Other clinical studies have demonstrated that SPV is a useful index to characterize lung and breast tumor vascularisation [56][57][58], but, for all we know, there are not studies about SPV use in liver tumor analysis. Moreover there are not study about the consistency of the index and the problem related to technical aspect.

5.2 SOURCES OF VARIABILITY IN THE USE OF STANDARDIZED PERFUSION VALUE FOR HCC STUDIES

We believe that could be helpful to employ Standardised Perfusion Value (SPV) in HCC perfusion studies which has the potential to be a useful non-invasive marker of angiogenesis. However, before using SPV in clinical practice, we need to verify its reliability. There are different causes of variability in applying the SPV index, e.g., the technical specifications of the CT system employed

and the image processing system. In this chapter we analyse the variability of the BFa estimates and the variability due to the calibration procedure of the CT system, this with the objective of verifying how these factors affects SPV values.

5.2.1 MATERIAL AND METHODS

The results are obtained from perfusion MDCT images of seventeen HCC patients. The algorithm, based on maximum slope method, presented in Chapter 4 was used to compute BFa and then SPV values.

According to SPV formula proposed by Miles we introduce BFa parameter computed with our algorithm based on slope method as Pt parameter.

As it can see by the following equation

$$35.SPV = \frac{BF_a \times W}{\frac{D}{\int a(t)}}$$

before the evaluation of SPV, BFa value has to be computed. In this phase, important causes of variability are slice and ROI selection [59].

5.2.2 ANALYSIS OF BFA VARIABILITY DUE TO ROI MANUAL SELECTION

Four expert radiologists (each with at least two years of experience in CT perfusion) were involved in the processing of the perfusion image data set for each patient. They were instructed to choose a single slice, from the perfusion image data set, that best depicted the tumor. Then, a circular ROI was drawn on the image displayed by the software, this was done in order to include as much of tumour tissue as possible, still remaining within its boundaries, and to ensure that it did not include large vessels. Once the slice is selected, different circular ROI of different size and in different position (respecting the inclusion criteria) can be selected on the same patient. Therefore, to evaluate the variability related to operator-dependent ROI selection, each radiologist, repeated, on the same selected slice and a week apart from each other, the input procedure (i.e. ROI position and dimension) four times on the same image set. For each set of measures (same radiologist and same

patient) mean value and standard deviation of BFa values were computed, finally providing the percentage of variation coefficient as a concise estimation of variability.

5.2.3 CALIBRATION OF THE CT SYSTEM

To evaluate the SPV index, the computation of the calibration K factor of the CT system was necessary (please see equation 35) . K factor is defined as the slope of the plot of attenuation in HU vs different con-trast agent concentrations (in milligrams per millimetre) [56]. Therefore, the calibration procedure aims to deter-mine the calibration K factor that characterizes the linear relationship between the measured attenuation in HU and the concentration of contrast agent [60][61]. We have carried out a specific procedure to evaluate the dependence of the K factor from the position in the CT scan for our CT system.

We performed our calibration procedure with a cylindrical acrylic phantom (Fluke Biomedical) with five holes. The thickness of the phantom is 15 cm with di-iameter of 32 cm and contains five pipettes holes (A, B, C, D, E, see Figure 21), one in the centre and four around the perimeter, 90° apart and 1 cm from the edge. The inside diameter of the holes is 1.31 cm.

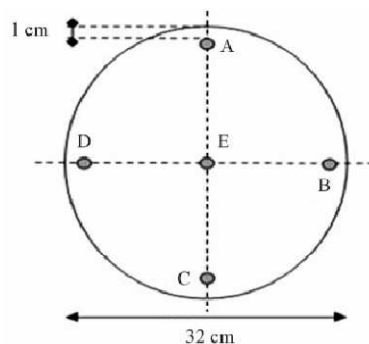


Figure 21: Scheme of the phantom used for the calibration procedure.

The phantom includes five acrylic inserts for plugging all the holes not filled with pipettes. Contrast agent of 400 mg/ml was diluted in physiological saline solution to obtain four different concentrations (6, 9, 12, 15 mg/ml). These concentrations correspond to physiological concentration in abdomen, liver, spleen and major vessels (such as aorta and vena porta) when a contrast agent bo-lus of 70 ml is injected at a rate of 4 ml/s. Pipettes with five different

concentrations of contrast were prepared (0, 6, 9, 12, 15 mg/ml). The scan parameters were the same used to obtain patients images in our HCC perfusion studies. The phantom was placed on the scanner table so that the pipettes of contrast agent were parallel to the z-axis of the CT scanner. The height of the table was adjusted in order to position the phantom at the centre of the CT gantry (Figure 22).



Figure 22: Example of phantom positioning into the CT gantry.

Our calibration protocol was based on six configurations (P0, PA, PB, PC, PD, PE) corresponding to different positions of the pipettes in the phantom. The evaluation of K factors in different configurations aims to estimate its dependence on the position in the scan field. In configuration P0, the five pipettes with different contrast concentrations (0, 6, 9, 12, 15 mg/ml respectively) were inserted in the five holes (A, B, C, D, E) of the phantom and then scanned simultaneously by means of a single acquisition using the perfusion protocol scan sequence. In the other configurations, the five pipettes were inserted one at a time in the same hole (i.e. A corresponding to PA, B to PB, C to PC, D to PD and E to PE configuration), and the others holes were filled with acrylic inserts. Therefore, for these configurations, five scans were necessary, each of them with a different

contrast agent concentration in the pipette, in order to estimate the K factor corresponding to every position. Since each TC scan provides 8 images, 8 K factors and their mean and standard deviation were computed for each configuration. To determine the K factor, regions of interest (ROI) were located by the operator on images in correspondence with each pipette containing contrast agent. The dimensions of the ROI were chosen as large as possible and avoiding partial volume effects and air bubbles generated during preparation of the solutions. For each contrast agent concentration, the mean values of gray levels (HU units) in each ROI were obtained in the different images. The slope of a linear least square fit of the five points (HU vs milligrams per milliliter) gave the calibration factor.

5.2.4 RESULTS

Results obtained about the estimation of variability in BFa evaluation are shown in Table 6.

	<i>Radiologist 1</i>			<i>Radiologist 2</i>			<i>Radiologist 3</i>			<i>Radiologist 4</i>		
	μ_1	(σ_1)	RSD ₁	μ_2	(σ_2)	RSD ₂	μ_3	(σ_3)	RSD ₃	μ_4	(σ_4)	RSD ₄
Patient 1	86.5	(4.9)	5.7	87.3	(15.2)	17.4	86.3	(4.0)	4.6	88.6	(1.5)	1.7
Patient 2	91.7	(4.7)	5.1	89.0	(3.7)	4.2	89.3	(4.0)	4.5	85.9	(5.1)	5.9
Patient 3	96.4	(0.6)	0.6	94.5	(1.5)	1.6	89.3	(12.8)	14.3	98.3	(2.5)	2.5
Patient 4	102.3	(4.6)	4.5	81.4	(14.0)	17.2	96.1	(23.4)	24.3	99.9	(2.4)	2.4
Patient 5	80.3	(2.3)	2.9	74.1	(6.4)	8.6	81.6	(1.3)	1.6	85.1	(3.1)	3.6
Patient 6	95.9	(1.1)	1.1	98.8	(30.6)	31.0	103.5	(7.1)	6.9	92.22	(16.4)	17.8
Patient 7	92.1	(2.2)	2.4	89.4	(1.5)	1.7	87.0	(2.9)	3.3	78.4	(5.9)	7.5
Patient 8	94.6	(0.8)	0.8	91.1	(1.3)	1.4	79.9	(15.3)	19.1	83.7	(14.2)	17.0
Patient 9	113.1	(2.0)	1.8	113.3	(1.8)	1.6	113.4	(2.9)	2.6	105.0	(9.5)	9.0
Patient 10	72.7	(0.9)	1.2	69.4	(12.0)	17.3	73.2	(1.1)	1.5	71.8	(4.7)	6.5
Patient 11	88.7	(1.0)	1.1	87.3	(3.5)	4.0	103.0	(9.3)	9.0	89.6	(0.6)	0.7
Patient 12	91.2	(1.7)	1.9	93.1	(2.0)	2.1	92.6	(1.4)	1.6	89.8	(2.0)	2.2
Patient 13	99.8	(3.1)	3.1	96.6	(10.8)	11.2	101.8	(6.6)	6.5	90.1	(5.4)	6.0
Patient 14	70.0	(21.5)	30.7	84.1	(23.4)	27.8	82.3	(5.4)	6.6	86.5	(8.0)	9.3
Patient 15	60.7	(1.8)	3.0	61.0	(0.5)	0.8	60.4	(1.7)	2.8	57.3	(4.3)	7.5
Patient 16	81.4	(1.4)	1.7	78.4	(2.1)	2.7	79.1	(6.4)	8.1	68.1	(1.5)	2.2
Patient 17	95.8	(2.6)	2.7	89.8	(6.5)	7.2	96.5	(4.8)	5.0	95.5	(2.7)	2.8

Table 6: Results obtained by the four radiologists in BFa estimation shown as average (μ), standard deviation (σ) and coefficient of variation in percentage (RSD)

They indicate that BFa computation is affected by the different ROI positioning made by the four operators. In fact, we obtained a great variability both among radiologists for the same patient (please, see different μ values along the lines) and among results obtained by the same radiologist on the same patient (please, see σ values).

We computed also RSD as estimation of variability observer-dependent, obtaining a mean value of 6.7%.

About the calibration procedure, we found that K factor depends on the position in the CT gantry. Obtained statistical parameters are shown in Table 7 (RSD less than 3%).

	μ	σ	RSD	Min	Max
K factor	35.9	1.0	2.8	34.6	37.0

Table 7: Statistics of K factor computed by means of the extended calibration procedure implemented by the authors

Finally, we have preliminarily estimated SPV index reference values, by computing them from CT perfusion exams in the group of seventeen HCC patients obtaining values in the range 8.0 - 18.3 [62]

5.2.5 DISCUSSION

Contrast-enhanced CT, in clinical practice, is frequently considered as the primary mean for assessing the therapeutic response of HCC to loco-regional treatments, especially after the introduction of multislice systems [63][64][65]. The CT perfusion technique is quickly spreading in the field of oncology since it can be simply incorporated into routine CT protocols, providing precious information about tumour grade and angiogenesis monitoring “in vivo” [50]. However, beneficial, extensive clinical application of perfusion CT requires a reliable use of the technique. In particular, when it is used for monitoring effects of a therapy, the reproducibility of the technique has to be such that the difference between repeated measurements is small compared to the

variability due to therapeutic changes [50]. At the moment, there are encouraging preliminary findings about reproducibility of the methodology and intra- and inter-observer variability but they regard only some body regions [66], not including the liver.

Software packages involving SPV computation are considered as advantageous in oncological applications [50], but we believe that the first application of SPV index to liver tumor is described here. At the best of our knowledge, in fact, there are no studies about SPV application in HCC patients, although perfusion CT studies are widely used in characterization of liver tumor. We believe that SPV index could be very helpful in liver tumor studies, nevertheless its application in clinical practice requires a preliminary evaluation of its reliability. In this study we wanted to provide details about some limitations of this technique.

Important is, for example, the variability in SPV computation. SPV index, normalised respect to CO and patient's weight was proposed by Miles [56] to reduce variability relative to these parameters. However, as can be seen from Equation (35), there is still variability due to K and BFa calculation. BFa computation is mainly related to the subjective positioning of the ROI done by a specific operator. Our results are in accordance with other works in which is reported the variability of the perfusion parameter, related to the processing analysis of perfusion image [66][67].

The positioning of the ROI consists in manually drawing a circular ROI along tumor margins so to allow the software to quantify perfusion values within it. It is crucial that the ROI is placed within tumor margins in all perfusion scan images. By consequence, all images of the study should be carefully analyzed, preferably in cine-loop modality, to ensure that the ROI does not extend beyond tumour margins and does not include vessels, air or surrounding adipose tissue in any of them. However, this procedure does not solve problems relative to patient movements during the time of acquisition. In fact, it is very difficult to choose a ROI that remains still on the tumor in each different image. The solution could be the selection of a different ROI for each image; however, this procedure can be boring for the operator, is time consuming and could introduce other sources of variability. Therefore, generally (as done also for this research work), once drawn a ROI, it should

be placed in the same position on all the temporal images of the same anatomical level [45]. Because of respiratory misregistration, which represents an important source of error, as reported also by other authors, it is possible that the selected ROI can include, in some slices, not only the tumor but also air, bone or normal liver parenchyma.

The calibration of CT systems is a necessary procedure, being the K factor a parameter included in the formula for computing the SPV.

Calibration factor depends on the specific CT system and on the acquisition parameters (KVp, mAs, kernel reconstruction) and changes over time. Some authors [68] proposed to compute K factor for each patient. Others [60] stated that it would be prudent to calibrate the CT system on the same day for each quantitative contrast- enhanced study.

However, we consider this recommendation a limit in clinical practice, because of the time needed to calibrate the system. Therefore, in order to verify if it is possible to avoid a complex calibration procedure, we estimated the contribution of K factor variability to the variability of SPV index respect to the variability due to BFa evaluation.

Calibration factor variance, due to the position in the gantry, resulted less than BFa variability (which is more than the double). So, we concluded that, if the daily calibration is preferred, a simplified protocol, which neglects the dependence of K factor from the position, may be utilised.

Otherwise, also according to literature, we advice, to keep it on the safe side, that calibration procedure should be repeated about every two weeks for a specific CT system, before that the amount of K factor variation, reported in literature [60], becomes comparable with variability due to BFa estimation, found in our results.

Finally, concerning values of SPV index, we evaluated them in seventeen patients in order to preliminarily verify the accordance between obtained results and the theoretical hypothesis that, being HCC characterised by a higher vascularisation respect to other kinds of tumours, it should show higher SPV values. We retain to have obtained interesting results even though our patients number was not so large and a direct comparison with the SPV values in other organs was not

possible. In fact, as expected, we found high SPV values (8.0 - 18.3) that characterize the hyper-vascularised HCC lesion, respect to lung (range 1.13 - 10.36) [56] [57] and breast tumour (range 2.5 - 5.9) [58].

5.2.6 CONCLUSION

The application of SPV index in HCC tumor could have a great potential in the management of HCC patients. However, to ensure the reliability of SPV perfusion index, it is advisable to use always the same acquisition protocol and to calibrate the CT system with the same measurements conditions at least every two weeks. Nevertheless, we have demonstrated that this aspect can be neglected until the intrinsic variability of perfusion parameter computation will be reduced.

In conclusion, we suggest the use of SPV index since CT perfusion provides qualitative assessment of vascularisation and therapeutic effects whereas a quantitative evaluation can be more useful. The use of SPV Index could be a feasible and non-invasive tool in the management and follow up of TACE/TAE, PEI, radiofrequency ablation and radioembolization treatment in HCC patients. This treatments are the most suited in patients with non surgical lesions in early, intermediate and advanced stage [69]. The response to these loco-regional treatments may be evaluated by comparing the difference in SPV values pre- and post-treatment.

The results of this work represent, in our opinion, an important step in the evaluation of the use of SPV index in liver tumor perfusion studies. However, we aware that the main limitation of our study is the small volume of coverage related to the image CT system. This volume is limited along the z-axis by the number of CT detectors used (e.g. 2.4 cm for our 16-slice CT system). Anyway, 16 slices CT systems are still widely spread and applied in the follow up of HCC patients [17].

6. PERFUSION MAPS

We have seen that evaluation of quantitative parameters about tumor perfusion, such as blood flow, by CT perfusion is gaining acceptance in clinical applications. “ROI based” analysis can be considered the gold standard technique to derive quantitative parameters, although it does not allow to depict the heterogeneous vascularisation of tumor tissue. On the contrary, “pixel by pixel” analysis, which has this potentiality, leads only to qualitative depiction of tumor perfusion by means of colour scale since still lacks of robust processing methods. In this chapter, we propose an algorithm for parametric estimation (pixel by pixel) of BFa values and used it for the analysis of a group of seventeen patients with primary liver tumour. Then, we compared obtained BFa values with those estimated by a “ROI based” approach, by using the same image processing, to investigate the reliability of parametric maps computed with the algorithm developed. Then an analysis by a “map based” approach was conducted to compare the performances of pixel by pixel MS and DOCM algorithm.

6.1 ROI APPROCH VS PIXEL BY PIXEL APPROACH: THE VALUE OF PERFUSION MAP

In literature, the first techniques, used for quantitative perfusion evaluation, were based on analysis of average HU variation in regions of interest (ROIs), identified manually on the functional images [10][27][30]. However, perfusion may be heterogeneously distributed and information regarding the differences may in this way be lost. In order to obtain more detailed information about perfusion, several attempts have been made to apply the kinetic calculations to individual pixel data and the generated distribution map is often referred to as a parametric image [22][41][70]. Nevertheless, parametric maps had initially only a qualitative value, because they were used just to help the radiologist in ROI positioning without validation of employed processing, so that their reliability as tool for quantitative estimation of perfusion parameters is still matter of debate. Pixel by pixel

analysis leads to high variance of the estimates and variance reduction by posterior spatial averaging produce variable results.

As we have seen in chapter 3, pixel TAC is noisier than ROI TAC because of the effect of photon noise. When generating TAC from very small regions or individual pixel, photon noise, in fact, becomes an important consideration. Random variations in photon numbers cause variability in measured attenuation values and hence, errors in the calculated perfusion values [20]. The problem of liver perfusion CT map processing is minimally addressed by other authors at the best of our knowledge. However some authors have published detail about parametric mapping algorithm in liver and myocardial perfusion MRI studies [51][71] and cerebral perfusion CT studies. When processing pixel TACs we have different problem than ROI TAC processing. First of all we have applied gamma fitting to pixel TAC. Our results showed that this fitting is not applicable because of the height noise. Gamma model, in fact, is adapted to represent the first part (upslope) of liver TACs and represent the dynamic phenomenon of contrast input with a single upslope. The experimental analysis of pixel liver and tumour TAC have demonstrated that there are two upslope related to arterial and portal phase. Gamma equation is not a good model for the pixel data. Spline interpolation is always applicable to pixel TAC but the problem is that pixel TAC are noisier than ROI TAC and the algorithm to remove outlier (proposed and applied to ROI TAC) don't give good results. Pixel spline interpolation is more affected by the noise than TAC spline interpolation and this cause map of poor quality that not simple allow ROI positioning.

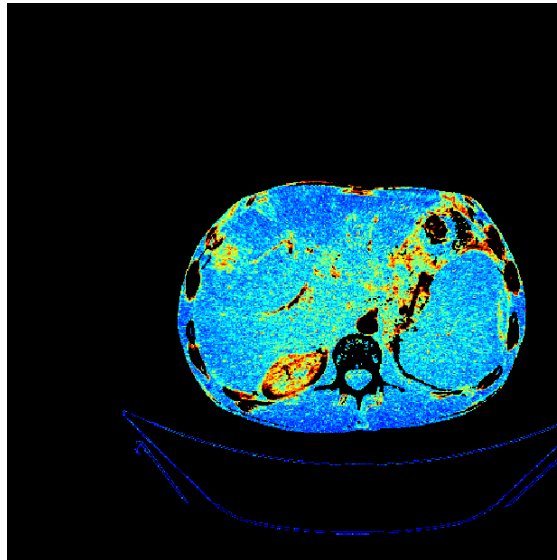


Figure 23: BFa map obtained with slope method algorithm

Moreover quantitative value obtained with spline fitting map overestimate arterial Blood Flow in primitive liver tumours (mean value in seventeen HCC patient is 320 ml/min/100ml). Our results suggest that a more reliable algorithms have to be investigated to obtain quantitative and qualitative map of BFa in liver tumour.

In this thesis we introduce an algorithm for parametric estimation (pixel by pixel) of BFa values with slope method. Then, because ROI based approach can be considered the “gold standard” for quantitative values, a comparison with our proposed algorithm is made to assess the reliability.

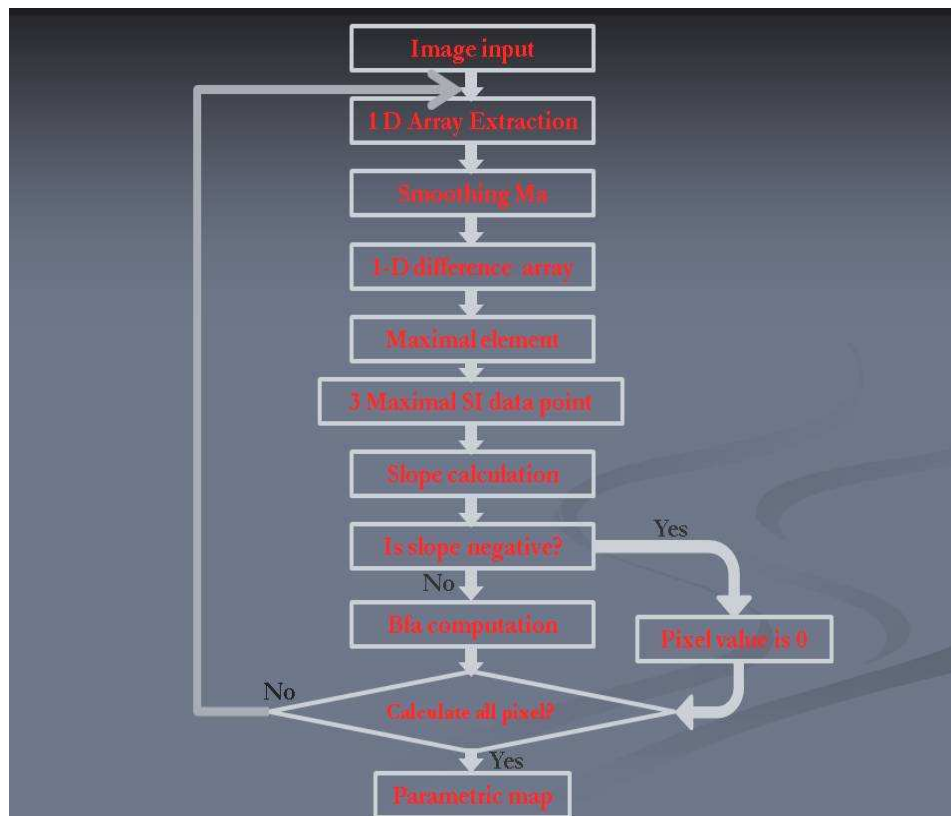


Figure 24 : Flow chart of algorithm used to obtain BFa map according to slope method

An analysis of correlation between perfusion parameters computed with a traditional ROI based approach and the values computed by means of a pixel-by-pixel map approach (using the same image processing technique) is presented.

According to literature [72], before analysis, a double threshold was imposed on the image set to exclude air and bone (only pixels included in the range $-50 \div 200$ HU were analyzed). For each CT perfusion image sequence of the liver tumour, the pixel values at each specific pair of coordinates in all the successive images were extracted to obtain a one dimensional HU array (1-D-array), which represents the pixel-TAC. This pixel-TAC was smoothed [36] with an average filter (5th-order moving-average filter), to reduce noise contribute. An array of differences (1-D-diff), which represents the contrast time variation, was then computed by the 1-D-array. Of course, the largest positive element in the 1-D-diff array corresponds to the maximum contrast positive variation. Three consecutive data points in the 1-D-array, centered around the element corresponding to the largest element identified in 1-D-diff, were then considered. The three consecutive points were

fitted using a linear curve fitting model. The slope of the regression line was considered as the maximum slope of the pixel-TAC. The procedure was repeated for calculating the up-slope of each pixel over the whole image. Thus, the image series was reduced to a single image (a parametric map) where each pixel value corresponds to the maximum up-slope of the TAC at that coordinates. According to Miles [50], dividing the parametric map by the maximum value of aorta-TAC (computed in a traditional way), we obtained the BFa parametric map. To compute BFa mean, variance and maximum values, a circular ROI was placed on the map in correspondence of the tumour region. The ROI was chosen to include the largest possible part of the tumour tissue, while remaining within its boundaries, and to ensure that it did not include large vessels. The same ROI choose for the map approach was drawn on the image of the tumour in the CT perfusion images. The mean of HU values inside the ROI were computed for each slice of the sequence to compute a mean tumor TAC. The processing used for the map approach was applied to this mean curve to obtain BFa values. BFa values computed using the map approach were plotted against BFa values computed by means of the ROI approach. The regression line shows the agreement between these values (Goodness of fit: SSE: 194.1 R-square: 0.90 Adjusted R-square: 0.89 RMSE: 3.6).

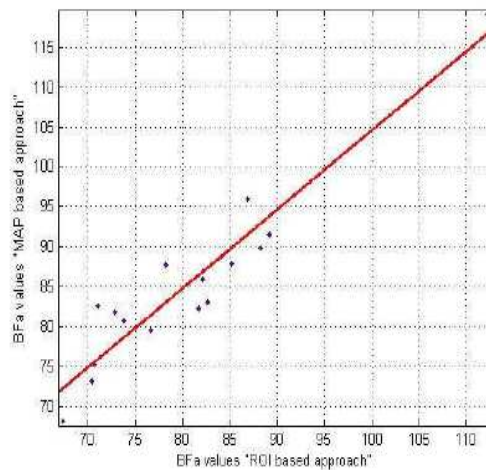


Figure 25: Correlation analysis between BFa values obtained with “ROI based” and “map based” approach

Anyway, the values obtained from the map were on average higher than those obtained from the ROI approach. That could probably due to the greater effect of the noise on the processing of the pixels-TAC. In fact, the presence of breathing, even if gentle, during dynamic imaging, did cause local errors in BFa estimation due to the movement of small structures between consecutive time slices, especially around the time of contrast arrival. This effect is a minor problem for ROI approach, probably for the effect of the mean operation inside the ROI. The R value obtained supports the idea that the use of an adequate processing permits to obtain reliable BFa maps compared with the ROI approach. Assessment of quantitative parameters by CT perfusion maps is still an open issue although the wide spread of perfusion technique in clinical practice. We have developed and tested in a group of 17 HCC patients an algorithm based on slope method to obtain perfusion maps . The results are in accordance with those obtained with a traditional ROI approach, using the same image processing algorithm. This suggests that the developed algorithm could give useful quantitative information about tumour heterogeneous hypervascularisation.

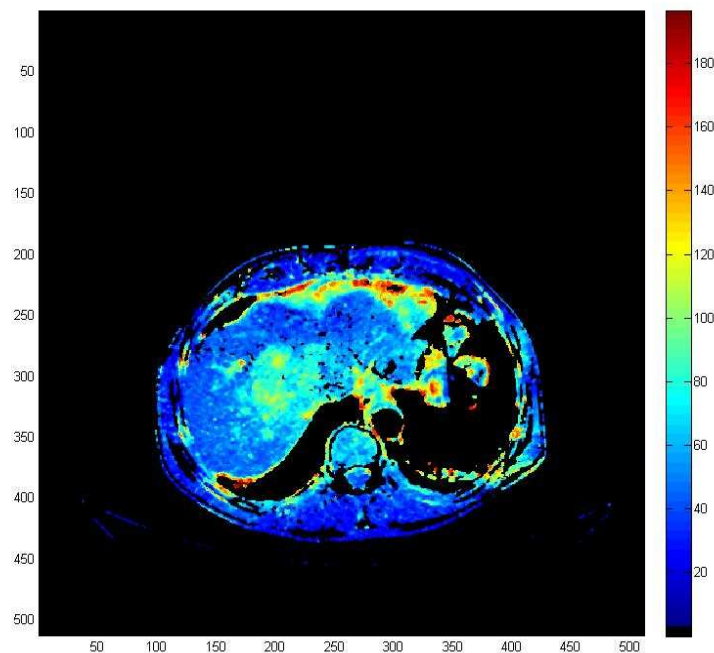


Figure 26: A BFa map obtained with the developed slope method algorithm

6.2 COMPARISON OF MAXIMUM SLOPE METHOD AND DUAL-INPUT-ONE-COMPARTMENT-MODEL: MAP BASED APPROACH

In this section we analyze and compare algorithms based on slope method (MS) and dual-input-one-compartment-model (DOCM) analytical model to obtain perfusion map. We have seen that DOCM requires that in volume of acquisition portal vein have to be always included and this aspect make it not always applicable. On the contrary DOCM is independent from injection rate of contrast agent. Our preliminary comparison based on a “ROI based approach” have demonstrated that DOCM method seems to be more robust to noise (see Chapter 4).

A new algorithm based on Linear least squares method (LLSM) was developed to process pixel by pixel perfusion CT map according to DOCM [54].

The images of the same five patient were processed with DOCM and MS algorithm (described in the above paragraph). Quantitative values to compare two algorithm are reported in term of mean and standard deviation of BFa pixel values inside the same ROI (positioned in a region of normal perfusion) reproduced on the two different maps (table 8)

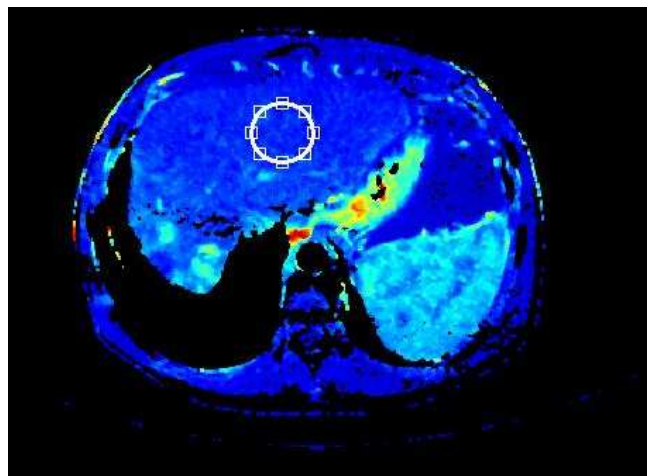


Figure 27: Positioning of a ROI on a region of liver parenchima characterized by normal vascularization

Patient	BF _a MS(ml/min/100ml)		BF _a DOCM(ml/min/100ml)	
	μ	σ	μ	σ
N° 1	39,45	5,210	31,68	30,32
N° 2	44,87	13,60	28,55	29,56
N° 3	62,32	7,684	27,32	18,77
N° 4	57,16	6,881	26,36	25,86
N° 5	64,94	15,86	17,63	12,70

Table 8: BF_a values computed with MS and DOCM algorithms. μ and σ are respectively the mean and the standard deviation of pixel values inside the ROI

Because the ROIs were positioned in a region of liver parenchyma characterized by uniform vascularisation to compare the two algorithm SNR was defined as the ratio of μ and σ (table 9)

Patient	SNR - MS		SNR - DOCM	
	μ/σ	$10\log \mu/\sigma$	μ/σ	$10\log \mu/\sigma$
N° 1	7,572	8,792	1,045	0,191
N° 2	3,299	5,184	0,966	-0,150
N° 3	8,110	9,090	1,456	1,632
N° 4	8,307	9,194	1,019	0,082
N° 5	4,095	6,123	1,388	1,434

Table 9: Results reported in term of SNR

The analysis of results demonstrate that SNR values associated to MS are lower than those calculated for DOCM. It means that slope method algorithm is preferable to compute quantitative BFa maps.

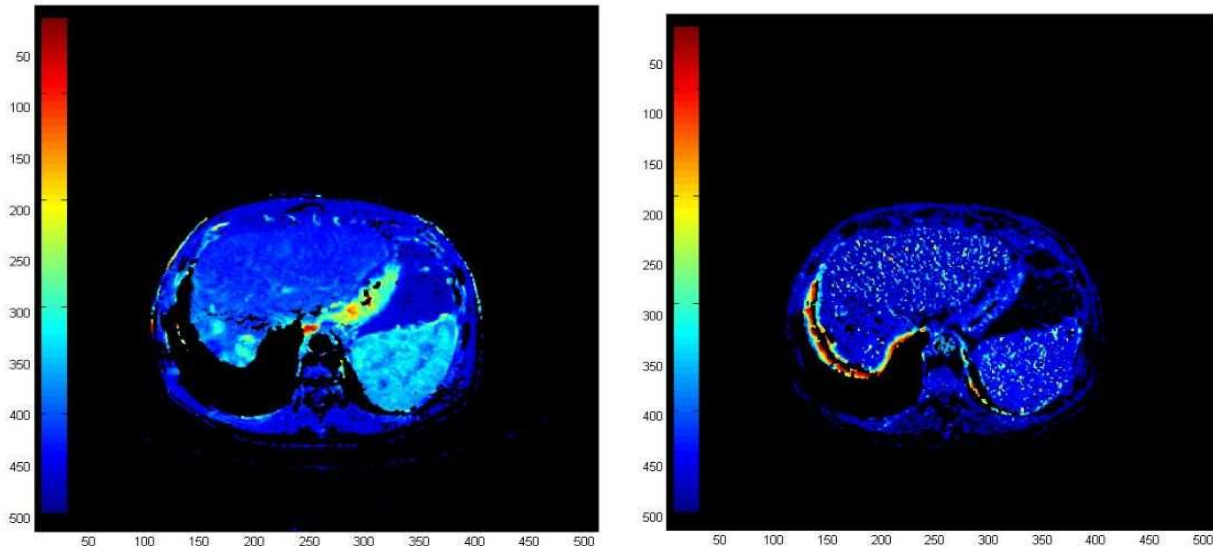


Figure 28: BFa map computed on the same patient with MS and DOCM algorithms

The analysis of BFa maps showed that even from the qualitative point of view the MS method (image on the left) is more reliable: in the right image (DOCM) the tumour is not visible and the spleen appears to be perfused as the liver parenchyma in the arterial phase (in opposition with the physiological processes of abdominal perfusion).

7. CONCLUSION

Improved therapeutic options for hepatocellular carcinoma place greater demands on surveillance tests for liver disease. Existing diagnostic imaging techniques provide limited evaluation of tissue characteristics beyond morphology; perfusion CT imaging of the liver has potential to improve this shortcoming. Perfusion parameters can be obtained applying mathematical model to TAC, i.e. contrast agent evolution over the time in a specific ROI positioned on the images. However, there are still some difficulties for an accurate and absolute quantification of perfusion parameters due, for example, to algorithms employed, to tracer kinetic modelling methods, to patient's weight and cardiac output, to the acquisition system.

In this thesis, new parameters or methods of interpretation and alternative methodologies about liver perfusion CT are presented in order to further investigate the potential and the limits of this technique.

Firstly analysis were made to assess the variability related to the mathematical model used to compute BFa values. Results were obtained implementing algorithms based on MS and DOCM. Statistical analysis on simulated data demonstrated that the two methods are not interchangeable regardless of the signal to noise ratio. Anyway slope method is the most used model to obtain perfusion parameters and allow to compute BFa values always when portal vein is not visible in perfusion CT scan.

Then variability related to TAC processing in the application of slope method is analyzed. Our aim was to find an automatic and reliable algorithm to compute TAC maximum slope after TAC processing. A fifth order smoothing with an automatic algorithm (that calculate the straight line fitting three points corresponding to TAC maximum increase) give the best results compared with manual selection.

Variability related to the patient, to the acquisition system and to the operator which select the ROI on the images are than analyzed. The consistency of SPV index was evaluated and a simplified calibration procedure was proposed. The application of SPV index allow to identify a clinical range to characterize HCC. At the end the quantitative value of perfusion map was analyzed. ROI approach and map approach provide related values of BFa and this means that pixel by pixel slope method algorithm give reliable quantitative results. Also in pixel by pixel approach MS algorithm present results uncorrelated with DOCM. Moreover DOCM method give quantitative results characterized by lower SNR value.

In conclusion, although it presents some limitation in the post-processing analysis, liver perfusion CT techniques are becoming an important tool in the medical research and clinical practice. The development of new automatic algorithm for a consistent computation of BFa and the analysis and definition of simplified technique to compute SPV parameter, would improve the clinical and scientific information provided by liver perfusion CT analysis.

REFERENCES

1. Pandharipande PV, Krinsky GA et al. Perfusion Imaging of the Liver: Current Challenges and Future Goals. *Radiology* 2005; 234: 661-673.
2. Folkman J, P Cole et al. Tumor behavior in isolated perfused organs: in vitro growth and metastases of biopsy material in rabbit thyroid and canine intestinal segment. *Ann Surg* 1966; 164:491–502.
3. Folkman J. The role of angiogenesis in tumor growth. *Semin Cancer Biol* 1992; 3:65–71.
4. Folkman J. Role of angiogenesis in tumor growth and metastasis. *Semin Oncol* 2002; 29:15–18.
5. Park YN, Yang CP et al. Neoangiogenesis and sinusoidal “capillarization” in dysplastic nodules of the liver. *Am J Surg Pathol* 1998; 22:656–662.
6. Roncalli M, Roz E et al. The vascular profile of regenerative and dysplastic nodules of the cirrhotic liver: implications for diagnosis and classification. *Hepatology* 1999; 30:1174–1178.
7. Krinsky GA, Theise ND et al. Dysplastic nodules in cirrhotic liver: arterial phase enhancement at CT and MR imaging: a case report. *Radiology* 1998; 209:461–464.
8. Krinsky GA, Zivin SB et al. Low-grade siderotic dysplastic nodules: determination of premalignant lesions on the basis of vasculature phenotype. *Acad Radiol* 2002; 9:336–341.
9. Park YN, Kim YB, et al. Increased expression of vascular endothelial growth factor and angiogenesis in the early stage of multistep hepatocarcinogenesis. *Arch Pathol Lab Med* 2000; 124:1061–1065.

10. Zhao J, Hu J et al. Vascular endothelial growth factor expression in serum of patients with hepatocellular carcinoma. *Chin Med J(Engl)* 2003; 116:772–776.
11. Chao Y, Li CP et al. Prognostic significance of vascular endothelial growth factor, basic fibroblast growth factor, and angiogenin in patients with resectable hepatocellular carcinoma after surgery. *Ann Surg Oncol* 2003; 10: 355–362.
12. K. A. Miles. Perfusion CT for the Assessment of Tumour Vascularity: Which Protocol?. *The British Journal of Radiology* 2003; 761(1):S36-S42.
13. D. V. Sahani, N. Holalkere et al. Role of Perfusion CT in Monitoring Anti-Angiogenic Response in Patients with Advanced Hepatocellular Carcinoma. *Contrast Media and Molecular Imaging* 2006; 1 (2): 72-72.
14. G. Chen, D.-Q. Ma et al. Computed Tomography Perfusion in Evaluating the Therapeutic Effect of Transarterial Chemoembolization for Hepatocellular Carcinoma. *World Journal of Gastroenterology* 2008; 14 (37): 5738-5743.
15. Z. Kan, S. Phongkitkarun, et al. Functional CT for Quantifying Tumor Perfusion in Antiangiogenic Therapy in a Rat Model. *Radiology* 2005; 237 (1): 151-158.
16. Z. Kan, S. Kobayashi et al. Functional CT Quantification of Tumor Perfusion after Transhepatic Arterial Embolization in a Rat Model. *Radiology* 2005; 237 (1): 144-150.
17. Sahani DV, Holalkere NS et al. Advanced hepatocellular carcinoma: CT perfusion of liver and tumor tissue--initial experience. *Radiology* 2007; 243(3):736-43.
18. Byung Ihn Choi. Advances of Imaging for Hepatocellular Carcinoma. *Oncology* 2010;78 (Suppl. 1):46-52.
19. Ippolito, D., Sironi et al. Perfusion computed tomographic assessment of early hepatocellular carcinoma in cirrhotic liver disease: initial observations. *Journal of computer assisted tomography* 2008; 32(6): 855-858.

20. K. A. Miles, M. P. Hayball et al. Functional images of hepatic perfusion obtained with dynamic CT. *Radiology* 1993; 188:405–411.
21. M. J. Blomley, R. Coulden et al. “Liver perfusion studied with ultrafast CT”. *J Comput Assist Tomogr* 1995; 19:424–433.
22. Y. Tsushima, S. Funabasama et al. Quantitative perfusion map of malignant liver tumors, created from dynamic computed tomography data. *Acad Radiol* 2004; 11: 215-223.
23. H. F. Yang, Y. Du et al. Perfusion computed tomography evaluation of angiogenesis in liver cancer. *Eur Radiol* 2010; 20: 1424–1430.
24. A. Komemushi, N. Tanigawa et al. CT perfusion of the liver during selective hepatic arteriography: pure arterial blood perfusion of liver tumor and parenchyma”. *Radiat Med* 2003; 21: 246-251
25. Peters AM, Brown J. et al. Non- invasive measurement of renal blood flow with ^{99m}Tc DTPA: comparison with radiolabelled microspheres. *Cardiovasc Res* 1987;21(11):830-4.
26. Peters AM, Gunasekera RD et al. Noninvasive measurement of blood flow and extraction fraction. *Nucl Med Commun* 1987;8(10):823-37.
27. Miles KA. Measurement of tissue perfusion by dynamic computed tomography. *Br J Radiol* 1991;64(761):409-12.
28. Miles KA, Hayball MP et al. Functional images of hepatic perfusion obtained with dynamic CT. *Radiology* 1993;188(2):405-11.
29. Miles KA, Hayball MP et al. Measurement of human pancreatic perfusion using dynamic computed tomography with perfusion imaging. *Br J Radiol* 1995; 68(809):471-5.
30. Blomley MJ, Coulden R et al. Liver perfusion studied with ultrafast CT. *Journal of Computer Assisted Tomography* 1995; 19(3):424-433.

31. Tsushima Y, Blomley MJK et al. Measuring portal venous perfusion with contrast-enhanced CT: comparison of direct and indirect methods. *Acad Radiol* 2002;9:276–82.
32. Materne R, Van Beers BE et al. Non-invasive quantification of liver perfusion with dynamic computed tomography and a dual-input one-compartmental model. *Clin Sci (Lond)* 2000; 99(6):517-25.
33. Van Beers BE, Leconte I et al. Hepatic perfusion parameters in chronic liver disease: dynamic CT measurements correlated with disease severity. *AJR Am J Roentgenol* 2001; 176: 667–73.
34. Cuenod CA, Leconte I et al. Deconvolution technique for measuring tissue perfusion by dynamic CT: application to normal and metastatic liver. *Acad Radiol*. 2002; 9(1):S205-11.
35. Axel L. Cerebral blood flow determination by rapid-sequence computed tomography. *Radiology* 1980; 137:679–686.
36. Bader TR, Grabenwöger F et al. Measurement of hepatic perfusion with dynamic computed tomography: assessment of normal values and comparison of two methods to compensate for motion artifacts. *Invest Radiol*. 2000; 35(9):539-47.
37. Roland Materne, Bernard E. et al. Hepatic perfusion after liver transplantation: non invasive measurement with dynamic single-section CT. *Clinical Science* 2000. 99: 517–525.
38. Adriëne Mendrik, Evert-jan Vonken et al. Noise filtering in thin-slice 4D Cerebral CT Perfusion scans. *Proc. of SPIE* 2010; 7623
39. Xin Liu, Andrew N. Primak et al. Quantitative evaluation of noise reduction algorithms for very low dose renal CT perfusion imaging. *Proc. of SPIE* 2009; 7258.

40. H. Bruder, R. Raupach et al. Spatio-temporal filtration of dynamic CT data using diffusion filters. Proc. of SPIE 2009; 7258.
41. Yoshito Tsushima, Shintaro Funabasama et al. Development of Perfusion CT software for personal computers. Academic Radiology 2002; 9 (8): 922–926
42. M. D'Anto, M. Cesarelli et al. Perfusion CT of the liver: slope method analysis. Proc. of GNB Conference, Torino, 2010.
43. Zhong, W. J. Wang et al. Clinical application of hepatic CT perfusion. World J Gastroenterol 2009; 15(8): 907-911.
44. Pina C. Sanelli, Gregory Nicola et al. Reproducibility of Postprocessing of Quantitative CT Perfusion Maps. AJR 2007; 188:213-218.
45. M. D'Antò, M.Cesarelli et al. Study of different Time Attenuation Curve processing in Liver CT Perfusion. Proc. of 10th IEEE International Conference on Information Technology and Applications in Biomedicine (ITAB), Corfù (Greece) 2010.
46. M. T. Madsen. A simplified formulation of the gamma variate function. Phys. Med. Bid. 1992; 1: 1597-1600.
47. M. Unser, Splines: A perfect Fit for Signal and Image Processing. IEEE signal processing magazine 1999; 16 (6): 22-38
48. T. R. Bader, A. M. Hemeth et al. Hepatic Perfusion after Liver Transplantation: Noninvasive Measurement with Dynamic Single-Section CT. Radiology 1998, 209: 129-134.
49. K. A. Miles. Functional computed tomography in Oncology. Eur J Cancer 2002; 38 (16) : 2079-84.
50. K.A. Miles, M.R. Griffiths. Perfusion CT: a worthwhile enhancement? BrJ Radiol 2003; 76: 220-31.

51. Chun Ruan, Scott Yang et al. First-Pass Contrast-Enhanced Myocardial Perfusion MRI Using a Maximum Up-Slope Parametric Map. *IEEE Transactions on Information Technology in Biomedicine* 2006; 10 (3): Page 574-580.
52. Vicky Goh, Steve Halligan et al. Quantitative Tumor Perfusion Assessment with Multidetector CT: Are Measurements from Two Commercial Software Packages Interchangeable? *Radiology* 2007; 242: 777-782.
53. Tomonori Kanda, Takeshi Yoshikawa et al. CT hepatic perfusion measurement: comparison of three analytic methods. *European Journal of Radiology* 2012; 81 (9):2075–2079.
54. S. Miyazaki, K. Murase et al. A quantitative method for estimating hepatic blood flow using a dual-input single-compartment model. *British Journal of Radiology* 2008; 81:790-800.
55. Masaya Miyazaki, Yoshito Tsushima et al. Quantification of hepatic arterial and portal perfusion with dynamic computed tomography: comparison of maximum-slope and dual-input one-compartment model methods. *Japanese Journal of Radiology* 2009; 27(3): 143-150.
56. Kenneth A. Miles, Matthew R. Griffiths et al. Standardized Perfusion Value: Universal CT Contrast Enhancement Scale that Correlates with FDG PET in Lung Nodules. *Radiology* 2001; 220: 548-553.
57. K. A. Miles, M. R. Griffiths et al. Blood Flow-Metabolic Relationships are Dependent on Tumour Size in Non-Small Cell Lung Cancer: A Study Using Quantitative Contrast-Enhanced Computer Tomography and Positron Emission Tomography. *European Journal of Nuclear Medicine and Molecular Imaging* 2005; 33 (1): 22-28.
58. Ashley M Groves, Gordon C Wishart, et al. Metabolic-Flow Relationships in Primary Breast Cancer: Feasibility of Combined PET/ Dynamic Contrast-

- Enhanced CT. *European Journal of Nuclear Medicine and Molecular Imaging* 2009; 36 (3): 416-421.
59. V. Goh, S. Halligan et al. Quantitative Assessment of Colorectal Cancer Tumor Vascular Parameters by Using Perfusion CT: Influence of Tumor Region of Interest. *Radiology* 2008; 247 (3): 726-732.
60. K. A. Miles, H. Young et al. Quantitative Contrast-Enhanced Computed Tomography: Is There a Need for System Calibration? *European Radiology* 2007; 17 (4): 919-926.
61. M. J. Siegel, B. Schmidt et al. Radiation Dose and Image Quality in Pediatric CT: Effect of Technical Factors and Phantom Size and Shape. *Radiology* 2004; 233 (2): 515-522.
62. Michela D'Antò, Mario Cesarelli et al. Sources of Variability in the Use of Standardized Perfusion Value for HCC Studies. *OJMI* 2012; 2 (2): 33-40
63. F. Fiore, P. Vallone et al. Levovist-Enhanced Doppler Sonography Versus Spiral Computed Tomography to Evaluate Response to Percutaneous Ethanol Injection in Hepato-cellular Carcinoma. *Journal of Clinical Gastroenterology* 2003; 36 (1): 63-67.
64. H. K. Lim, D. Choi et al. Hepatocellular Carcinoma Treated with Per-cutaneous Radio-Frequency Ablation: Evaluation with Follow-Up Multiphase Helical CT. *Radiology* 2001; 221 (2): 447-454.
65. I. R. Kamel, E. Liapi et al. Multidetector CT of Hepatocellular Carcinoma. *Best Practice & Research Clinical Gastroenterology* 2005; 19 (1): 63-89.
66. D. Fiorella, J. Heiserman et al. Assessment of the Reproducibility of Postprocessing Dynamic CT Perfusion Data. *American Journal of Neuroradiology* 2004; 25 (1): 97-107.

67. V. Goh, S. Halligan, et al. Quantitative Assessment of Colorectal Cancer Perfusion Using MDCT: Inter- and Intraobserver Agreement. *American Journal of Roentgenology* 2005; 185 (1): 225-231.
68. K. Takanami, S. Higano et al. Validation of the Use of Calibration Factors between the Iodine Concentration and the Computed Tomography Number Measured outside the Objects for Estimation of Iodine Concentration inside the Objects: Phantom Experiment. *Radiation Medicine* 2008; 26 (4): 237-243.
69. R. Wong, C. Frenette. Management of Hepatocellular Carcinoma: An Update *Hepatology* 2011; 53 (3): 16-24.
70. Petralia G., Preda L. et al. CT perfusion in solid-body tumours. Part I: technical issues *Radiol med* 2010; 115:843–857.
71. Zavaljevski Aleksandar, Holland Scott K. Et al. Multilevel computed hemodynamic parameter maps from dynamic perfusion MRI. *IEEE Transactions on Instrumentation and Measurement* 1999; 48 (3): 711- 720.
72. Y. Tsushima, Y. Unno et al. Measurement of human hepatic and splenic perfusion using dynamic computed tomography: a preliminary report. *Comput Methods Programs Biomed* 1998; 57: 143-146.